ACKNOWLEDGEMENTS

The support of the Director of the Centre for Building Studies, Dr. P.P. Fazio, in this research is acknowledged. Financial assistance was received through the team grant from la Formation de Chercheurs et d'Action Concertee (FCAC) and from NRC grant No. A7300.

The author acknowledges his indebtedness to Prof. Cedric Marsh and Dr. H.K. Ha, without whose guidance, advice and keen interest in this work, this thesis would not have been possible; the author will always be grateful.

Thanks are also due to Mr. Joseph Zilkha, Technician, Centre for Building Studies, Mr. Louis Stankevicius, Technical Officer, Civil Engineering Department and to Mr. Albert Carbone, Research Assistant, Mechanical Engineering Dept., for their valuable assistance.

I also thank Mrs. Pamela O'Cain for her time and efforts in the typing of this thesis.

To my parents and to my brother Mohamed.

TABLE OF CONTENTS

LIST OF FIGURES

NOTATIONS

{ }	A column vector
[ ]	Row vector, or rectangular or square matrix
$[\ ]^T$, $\{\ \}^T$	Transpose of a matrix or column vector
, (comma)	Indicates partial differentiation when used before a subscript, for example: $w_{,x} = \frac{\partial w}{\partial x}$; $v_{,zz} = \frac{\partial^2 v}{\partial z^2}$
E, ν	Elastic modulus and Poisson's ratio of an isotropic material. When integers are used as subscripts, 1 refers to aluminium skin and 2 to wood core of a sandwich panel.
E_{xx}, E_{zz}	The moduli of elasticity of orthotropic material in the x and z-directions respectively
ν_{xz}, ν_{zx}	Poisson's ratio of orthotropic material
G_{xz}	The shear modulus of orthotropic material
T	Temperature change from ambient
t	Thickness of a finite element
U_o	Strain energy
π	Total potential energy
u,v,w	Displacements of a point in the coordinate directions. Note, u is the skin displacement, v is the core displacement in the x-direction in mathematical analysis.
u(v),w	Are the nodal displacement in x, z-directions respectively in the finite element analysis
{d}	Nodal degrees of freedom for element

{D}	Strain displacement matrix, $\{\varepsilon\} = [D]\{d\}$
{P}	Concentrated loads applied to structure nodes.
$\{\sigma\}$ $\{\varepsilon\}$	Engineering stresses and strains
σ_x, σ_z	The normal components of stress parallel to x and z axes
τ	Shear stress
τ_b	Shear stress in glue line of sandwich panel
a,b	Linear dimensions of finite element in the x and z directions, respectively
α	Thermal expansion coefficient. Note: when integers are used as subscripts, 1 refers to skin, 2 to core materials of sandwich panel.
[E]	Elastic constants of orthotropic material.
θ	Shear strain.

CHAPTER I

INTRODUCTION

The American Society for Testing and Materials (ASTM), defines a structural sandwich as a construction comprised of a combination of alternating dissimilar simple or composite materials, assembled and intimately fixed in relation to each other so as to use the properties of each to specific structural advantages for the whole assembly [3]. The structural stressed skin is the family term for all structures where thin sheet coverings are major contributors to structural performance, other members are used to transfer stresses and stabilize the compression portions of the skins. Monocoque is more or less the same thing. It may refer to stressed skin enclosures where the sidewalls themselves are arranged as the shear webs [4].

The basic principle of spaced facings was discovered about 1820 by a Frenchman named Duleau. Panels utilizing asbestos board skins with vegetable fiberboard cores were used as early as World War I. During World War II the trend to more efficient use of labour and materials, particularly in aircraft, resulted in increasing use of panels. The development or adaptation of new materials, the majority of which are plastics, has made an impact on the field of sandwich construction. An example is the use of foams in building construction [1].

There has been a growing interest in many applications of composite or sandwich constructions. These developments are based on the concept, not of using or favoring any one material, but rather of employing any available material. It goes even further in that it

sets up for certain uses, desired requirements as to mechanical and physical properties that are not yet available in many materials. These objectives provided a target, as it were, for further development [2].

Another feature of sandwich construction is the opportunity, through efficient structural design, to stress each material to the practical limit of its possibilities.

The basic structural principle of a sandwich is much the same as that of an I beam, which is an efficient structural shape because as much as possible of the material is placed in flanges situated farthest from the neutral axis. Only enough material is left in the connecting web to make the flanges act in concert and to resist shear and buckling. In a structural sandwich the facings take the place of the flanges, and the core takes the place of the web. The difference is that the core of a sandwich is a different material from the facings, and it is spread out instead of concentrated in a narrow web. The facings act together to form an efficient internal stress couple or resisting moment counteracting the external imposed bending moment. The core resists the shear stresses set up by the external loads, and it has the further important function of stabilizing the facings against wrinkling or buckling (Fig. 1.1). It must, therefore, be strong and stiff enough to resist transverse tension and compression set up by the facings as they try to wrinkle. In direct compression, the same supporting action is important. A thin plate may buckle when an axial compressive stress is applied.

If it is made a part of a sandwich, lateral restraint against buckling is provided by the core, and the plate can withstand considerably higher compressive stresses. Evidently, the bond between facings and core must be strong enough to resist the shear and tensile stresses set up between them. The adhesive used to bond facings and core together is of critical importance [1].

Bowing and internal condensation can be particular, if unrelated, problems of sandwich constructions wherever differential temperature or moisture regimes exists across the panel thickness. The environmental ranges and effects should be briefly sketched before discussing material properties. In cold countries, the outer skin of an insulated panel (wall or roof) can be at -30°F while the inner skin is near 70°F, giving a 100°F differential. Similarly, in summer, the outer skin can reach 170°F for brief periods, or even higher with dark colours, while the inner skin is at, say, 70°F, again a 100°F differential. The amount of bowing, if unconstrained, assumed the same in either case, inward in the first case and outward in the second case [4].

There is still little information available on the thermal stresses in the sandwich panels, and most of the existing information is from experimental results. Panel failure, due to internal thermal stresses, is common and a theoretical solution for such stresses is required.

The true panel is three dimensional, but the anlaysis of the thermal stresses in sandwich panels is simplified by studying the behaviour of a unit width sandwich strip in two dimensions.

The materials used to form the sandwich specimens were white pine, aluminium 3003 and epoxy Bostik 7087.

The theoretical analysis has been done for many different boundary conditions and the finite element analysis for the case of a uniform temperature rise. The experiments were for the case of a free edge specimen.

Chapter II gives the mathematical derivations of displacements and stresses of sandwich panel components based on theory of elasticity. A computer programme was written to evaluate the Fourier series. In Chapter II also, is given the finite element programme used to determine thermal stress.

Chapter III deals with the experimental work, relevant equipment, test procedures and the results.

In Chapter IV, a comparison is made of the theoretical solution and the experimental results, and conclusions drawn.

CHAPTER II

THEORETICAL ANALYSIS

A sandwich panel exposed to a temperature change will expand or bow creating thermal stresses in the skins. The thermal stresses may be insignificant or important depending on the elastic properties of the core materials. For example, using wood as a core material results in higher thermal stresses than using plastic foam.

In the subsequent theoretical analysis the following assumptions are made:

1 - Skin thickness is small compared to that of the core.

2 - The sandwich panel has constant thickness.

3 - The skins are made from isotropic material.

4 - Deformation within the glue line is neglected.

5 - The wood core is orthotropic in x-z plane.

6 - Poisson's ratio of the core material is neglected.

7 - Constant temperature distribution on each skin.

8 - Constant temperature through the skin thickness.

9 - The sandwich panel is subjected to temperature difference only (the external load's and the panel's own weight are neglected).

10 - Only the coefficient of thermal expansion in the longitudinal direction of both skin and core are considered.

11 - The effect of variation in moisture content is neglected.

2.1 OVERALL BEHAVIOUR - APPROXIMATE SOLUTION

Consider a sandwich panel consisting of a core of thickness 2d and two faces each of thickness t (Fig. 2.1), subjected to temperature changes at the skins (Fig. 2.2).

The normal stress in the skin σ, can be expressed as follows [5]

$$\sigma_1 = \frac{T(\alpha_1-\alpha_2)}{t\left(\frac{1}{E_1 t} + \frac{1}{E_2 d}\right)} \qquad (2.1)$$ For uniform temperature change T.

$$\sigma_1 = \frac{T(\alpha_1-\alpha_2)}{t\left(\frac{1}{E_1 t} + \frac{3}{E_2 d}\right)} \qquad (2.2)$$ For $\pm T$ temperature gradient (edges free).

$$\sigma_1 = \alpha_1 \, T \, E_1 \qquad (2.3)$$ For $\pm T$ temperature gradient (panel kept flat).

in which α_1, E_1 and α_2, E_2 are the thermal expansion coeffidient and the modulus of elasticity of skin and core materials respectively.

In the above expression, it is assumed that the entire interacting load is transferred at the end as shown in (Fig. 2.2).

2.2 THEORETICAL ANALYSIS

For Core

The equilibrium equations of an infinitesimal, two dimensional element, (Fig. 2.3), are as follows:

$$\sigma_{x,x} + \tau_{zx,z} = 0 \text{ in } x\text{-direction*} \qquad (2.4)$$

$$\sigma_{z,z} + \tau_{xz,x} = 0 \text{ in } z\text{-direction} \qquad (2.5)$$

The strain-displacement relations for the same element give the following relationships in which v and w are the displacements along x and z axes respectively.

$$\sigma_x = E_{xx}\varepsilon_x = E_{xx}v_{,x} \tag{2.6}$$

$$\sigma_z = E_{zz}\varepsilon_z = E_{zz}w_{,z}^{*} \tag{2.7}$$

$$\tau_{xz} = G_{xz}\theta = G_{xz}(v_{,z} + w_{,x}) \tag{2.8}$$

2.2.1 UNIFORM TEMPERATURE RISE T (FREE EDGES)

Using the coordinate axes of the sandwich panel shown in Figure 2.4, equations (2.4),(2.6) and (2.8) give the equilibrium equation for an infinitesmial core element as follows:

$$v_{,xx}E_{xx} + G_{xz}(v_{,zz} + w_{,xz}) = 0 \tag{2.9}$$

$$w_{,zz}E_{zz} + G_{zx}(v_{,zx} + w_{,xx}) = 0 \tag{2.9a}$$

In order to obtain a solution it is assumed that the displacement w is negligible and to satisfy the following boundary conditions:

at	$x = 0$	$v = 0$	$v_{,z} = 0$
	$x = L$		$v_{,x} = 0$
	$z = 0$		$v_{,z} = 0$

the solution of equation (2.9) takes the following form:

$$v = \sum_{n=1,3}^{\infty} A_n \sin\left(\frac{n\pi}{2L}x\right) \cosh\left(\Gamma\frac{n\pi}{2L}\right) z \tag{2.10}$$

---

*, (comma) Indicates partial differentiation when used before a subscript.

where $\Gamma = (E_{xx}/G_{xz})^{\frac{1}{2}}$

For skin element, the stress equilibrium equation is

$$\tau_o = t\,\sigma_{1,x}$$

where $\sigma_1 = u_{,x}E_1$, u = axial displacement in the skin (2.11)

By using equations (2.8) and (2.11), shear stress in glue line can be represented as follows:

$$\tau_o = v_{,z}G_{z=d} \tag{2.12a}$$

$$= t\,\sigma_{1,x} \tag{2.12b}$$

$$\tau_o = tE_1\,u_{,xx} \tag{2.12c}$$

From equations (2.12a) and (2.12c), skin displacement is obtained [5] as

$$u = (G_{xz}\Gamma/tE_1)\sum_{n=1,3}^{\infty}(2LA_n/n\pi)\,\sin(n\pi x/2L)\,\sinh(\Gamma n\pi d/2L) \tag{2.13}$$

The strain compatibiltiy equation at the glue line (i.e. z=d) is:

$$-u + v_{z=d} = (\alpha_1 - \alpha_2)Tx$$

$$\sum_{n=1,3}^{\infty}\frac{A_n}{(\alpha_2-\alpha_1)TL}\left(\frac{2G_{xz}\Gamma L}{tE_1 n\pi}\sinh\frac{\Gamma n\pi d}{2L} + \cosh\frac{\Gamma n\pi d}{2L}\right)\sin\frac{n\pi x}{2L} = \frac{x}{L}$$

Using Fourier expansion of $\frac{x}{L}$ gives

$$A_n = \frac{8(-1)^{\frac{n-1}{2}}(\alpha_2-\alpha_1)TL}{(n\pi)^2\left(\frac{2G_{xz}\Gamma L}{tE_1 n\pi}\sin\frac{\Gamma n\pi d}{2L} + \cosh\frac{\Gamma n\pi d}{2L}\right)} \tag{2.14}$$

Having known equations (2.10), (2.12a), (2.12b) and (2.13), shear stress at the glue line and normal stress in the skin are as follows:

$$\tau_o = (G_{xz}\pi\Gamma/2L)\sum_{n=1,3}^{\infty} n\,A_n\,\sin(n\pi x/2L)\,\sinh(\Gamma n\pi d/2L) \tag{2.15}$$

$$\sigma_1 = (G_{xz}\Gamma/t) \sum_{n=1,3}^{\infty} A_n \cos(n\pi x/2L) \sinh(\Gamma n\pi z/2L) \tag{2.16}$$

2.2.2 TEMPERATURE GRADIENT ± T (FREE EDGES)

In this case, the panel will bow and the lateral deformation cannot be ignored. To satisfy the boundary conditions for this case, which are given below:

at	$x = 0$	$v = 0$	$v,z = 0$
	$x = L$		$v,x = 0$
	$z = 0$	$v = 0$	$v,x = 0$

The core displacement in x-direction is assumed to be given by:

$$v = \sum_{n=1,3}^{\infty} A_n \sin(n\pi x/2L) \sinh(\Gamma n\pi z/2L) \tag{2.17}$$

Equations (2.11) and (2.12a) cannot be applied in this case due to transverse displacement effect. Introducing internal equilibrium of stress, the internal moment is given by:

$$(2d)(t\sigma_1) - 2\int_0^d (z\sigma_x\, dz) = 0$$

Assuming linear stress distribution across the panel, the second term in the last equation is replaced by $\frac{2}{3} d^2 \sigma x_{z=d}$ and the skin displacement in x-direction takes the following form:

$$u = \frac{d\, E_{xx}}{3tE_1} \sum_{n=1,3}^{\infty} A_n \sin\left(\frac{\pi n x}{2L}\right) \sinh\left(\frac{\pi n \Gamma d}{2L}\right) \tag{2.18}$$

The strain compatibility equation at the glue line (i.e. z=d) is:

$$- u + v_{z=d} = (\alpha_1 - \alpha_2)Tx$$

$$\sum_{n=1,3}^{\infty} \frac{A_n}{(\alpha_2-\alpha_1)TL} \left(\frac{dE_{xx}}{3tE_1} \sinh \frac{\pi n \Gamma d}{2L} + \sinh \frac{\Gamma n \pi d}{2L}\right) \sin \frac{\pi n x}{2L} = \frac{x}{L}$$

$$\sum_{n=1,3}^{\infty} \frac{A_n}{(\alpha_2-\alpha_1)TL} \left(1 + \frac{dE_{xx}}{3tE_1}\right) \sinh \frac{\pi n \Gamma d}{2L} \sin \frac{\pi n x}{2L} = \frac{x}{L}$$

Using the Fourier expansion of $\frac{x}{L}$ gives

$$A_n = \frac{8(-1)^{\frac{n-1}{2}} (\alpha_2-\alpha_1)TL}{(\pi n)^2 (1 + \frac{dE_{xx}}{3tE_1}) \sinh \frac{\pi n \Gamma d}{2L}} \tag{2.19}$$

Shear stress in the glue line, eqn. 2.8 and 2.12b, is

$$\tau_o = (v_{,z} + w_{,x})\, Gxz = t\sigma_{1,x}$$

From which core displacement in z-direction will have the following form:

$$W = \sum_{n=1,3}^{\infty} \Gamma A_n \cos \{(\pi n x/2L)[(\pi n \Gamma d/6L) \sinh (\pi n \Gamma d/2L) - \cosh (\pi n \Gamma d/2L)]\} \tag{2.20}$$

By applying equations (2.11) and (2.8), shear stress in glue line and normal stress in skin can be represented by the following equations:

$$\sigma_1 = \left(\frac{\pi E_{xx} d}{6tL}\right) \sum_{n=1,3}^{\infty} n A_n \cos (\pi n x/2L) \sinh(\pi n \Gamma d/2L) \tag{2.21}$$

$$\tau_o = \frac{\pi^2 E_{xx} d}{12L^2} \sum_{n=1,3}^{\infty} n^2 A_n \sin(\pi n x/2L) \sinh(\pi \Gamma n d/2L) \tag{2.22}$$

2.2.3 EVALUATIONS AND ASSESSMENTS

Because there are many terms involved in displacement and stress formulas, equations (2.10), (2.13), (2.15), (2.16), (2.17), (2.18), (2.20), (2.21) and (2.22), a computer programme, Appendix A, was written to evaluate them.

Consider a sandwich panel of the following proportions:

$L = 18.0$ in.	$G_{xz} = 160{,}000$ psi
$t = .025$ in.	$d = .8695$ in.
$E_1 = 10{,}000{,}000.$ psi	$E_{xx} = 1{,}600{,}000$ psi
$\alpha_1 = .000013$ /°F	$\alpha_2 = .000003$ /°F

For different temperature changes, the final normal stress in the skin are shown in Figs. (2.5) to (2.10). Consider a uniform temperature change = 6.5°F, gradient temperature change = $\pm$ 17.83°F. The normal and shear stresses in the skin and the glue line respec. are evaluated using equations (2.1), (2.2), (2.11), (2.12C), (2.15), (2.16), (2.21) and (2.22). The results are shown in Fig. (2.11), (2.12). By using the superposition principle as shown in Fig. (2.13), the final stresses are shown in Fig. (2.14) and (2.15).

From Fig. (2.11) one can see that near the panel end the rate of slope change of the skin normal stress curve is higher in case of temperature gradient than in the case of uniform temperature rise, or in other words, the shear strains are highest in case of temperature gradient, eqn. 2.8, therefore, the net skin normal stress in this zone is governed by the normal stresses due to uniform temperature rise (the larger stress). This is the reason of stress changing sign near the panel end in the lower curve in Fig. (2.14).

2.3 FINITE ELEMENT ANALYSIS

2.3.1 ELEMENT STIFFNESS MATRIX DERIVATION

The basic concept of the finite element method is that a continuum can be modeled analytically through its subdivision into regions, the behaviour of each being uniquely described with the aid of either a stress or a displacement function. The technique has a theoretical basis within the framework of the classical theory and is related, by analogy, to the Ritz method used in the solution of elastomechanics problems.

While in the conventional Ritz procedure, one set of functions describes the displacement field in the entire continuum, the finite element method assumes individual displacement fields for each element, uniquely defined in terms of the displacements at the element's nodes or points of connection. Continuity is assured within the separate elements, and as such the whole domain can be regarded as piece-wise continuous. By definition, continuity is preserved at the nodes. In addition, a careful choice of displacement field can ensure continuity of deformations across element boundaries as well.

Research in the field of finite element idealization has produced a large number of basic elements to fit particular purposes or to be used in the solution of specific problems.

As the present work is concerned with the study of the transverse section of sandwich panel subject to in-plane loads, the search will be directed towards two-dimensional plane stress elements.

In this category, the rectangular element with a linear variation of displacements along the edges seems to be most suitable. This element, which ensures compatibility of deformations at the interfaces, has been shown to produce better results than the constant strain triangle or the quadrilateral formed by combining four such triangles.

To solve a problem in elasto-mechanics, one has to satisfy three types of conditions: geometric, physical and static. Once the displacement field has been assumed within an element, and expressed in terms of the nodal displacement $\underline{d}$, the strains $\underline{\varepsilon}$ are obtained by proper differentiation of the displacement functions. In symbolic form:

$$\{\varepsilon\} = [D]\ \{d\} \tag{2.23}$$

This constitutes the geometric relation of compatibility.

To express the physical nature of the problem, the constitutive relation linking stresses to strains is used

$$\{\sigma\} = [E]\ \{\varepsilon\} \tag{2.24}$$

Having formulated the first two conditions, the third one will have still to be satisfied. Since the displacement field must satisfy approximately the condition of equilibrium, the correct set of displacements should minimize the potential energy associated with element deformation.

To accomplish that, the first variation of the total potential with respect to the nodal displacement $\{d\}$ must have a stationary value. The strain energy U_o per element is

$$U_o = \int_{vol.} \frac{1}{2} \{\sigma\}\ \{\varepsilon\}\ d.vol.$$

$$= \int_{vol.} \frac{1}{2} \{d\} [D]^T [E] [D] \{d\} \, d\,vol. \tag{2.25}$$

The total potential energy π is, by definition

$$\pi = U_o - W_e$$

$$= U_o - \{P\}^T \{d\} \tag{2.26}$$

in which W_e = work done by the external forces.

Applying the first variation on (2.26) with respect to {d} and equating to zero

$$\frac{\partial \pi}{\partial \{d\}} = 0$$

we obtain a set of simultaneous linear equations in {d} such that

$$\{P\} = \int_{vol.} ([D]^T [E] [D] \; d\,vol.) \{d\} \tag{2.27}$$

or written in another form

$$\{P\} = [K] \{d\} \tag{2.28}$$

Where [K] is recognized as the stiffness matrix and {P} = the equivalent nodal force vector. The element nodal force P_i at node i can be expressed in terms of the applied temperature as

$$P_i = \frac{1}{2} \alpha T_i E_{xx} b \tag{2.29}$$

in which T_i = the temperature at node i, and b = the element width (Fig. 2.16).

The preceding formulation is a general step by step description of the derivation of a stiffness matrix for a finite element. More specifically, referring to Fig. (2.16) for the rectangular element, the displacement field within the element is defined by

For skin element

$$u = \left[(1-\frac{z}{b})(1-\frac{x}{a}) \quad (1-\frac{z}{b})\frac{x}{a} \quad \frac{xz}{ba} \quad \frac{z}{b}(1-\frac{x}{a})\right] \begin{Bmatrix} u1 \\ u2 \\ u3 \\ u4 \end{Bmatrix}$$

For core element, the same displacement field is considered by replacing u by v.

And in the z-direction:

$$w = \left[(1-\frac{z}{b})(1-\frac{x}{a}) \quad (1-\frac{z}{b})\frac{x}{a} \quad \frac{zx}{ba} \quad \frac{z}{b}(1-\frac{x}{a})\right] \begin{Bmatrix} w1 \\ w2 \\ w3 \\ w4 \end{Bmatrix}$$

in terms of the nodal freedom u_i and w_i at the corners 1, 2, 3 and 4.

Substituting ξ for $\frac{x}{a}$ and η for $\frac{z}{b}$, the [D] matrix relating the strains $\{\epsilon\}$ to the nodal freedoms $\{d\}$ takes the following form:

$$[D] = \begin{bmatrix} -\frac{1-\eta}{a} & 0 & \frac{1-\eta}{a} & 0 & \frac{\eta}{a} & 0 & \frac{-\eta}{a} & 0 \\ 0 & -\frac{1-\xi}{b} & 0 & -\frac{\xi}{b} & 0 & \frac{\xi}{b} & 0 & \frac{1-\xi}{b} \\ -\frac{1-\xi}{b} & -\frac{1-\eta}{a} & \frac{-\xi}{b} & \frac{1-\eta}{a} & \frac{\xi}{b} & \frac{\eta}{a} & \frac{1-\xi}{b} & \frac{-\eta}{a} \end{bmatrix}$$

The [E] matrix defining the constitutive relation between stresses and strains for orthotropic media, in two dimensions is

$$[E] = \frac{1}{(1-\nu_{xz}\nu_{zx})} \begin{bmatrix} E_{xx} & \nu_{zx}E_{xx} & 0 \\ \nu_{xz}E_{zz} & E_{zz} & 0 \\ 0 & 0 & (1-\nu_{xz}\nu_{zx})G_{xz} \end{bmatrix}$$

Since the thickness of the elements t is constant over the element, the stiffness matrix of equation (2.28) can be written [8] as

$$K = t \int_{vol.} [D]^T[E][D]\, dx\,dz$$

$$= t\, a\, b \int_0^1\int_0^1 [D]^T[E][D]\, d\xi\, d\eta$$

Performing the triple matrix product $[D]^T$ [E] [D], an 8 by 8 matrix is obtained populated by expressions which are functions of ξ and η. Integration of these expressions will lead to subsequent evaluation of the K_{ij} terms of the stiffness matrix [K].

After proper simplification, it is found that the 8 by 8 stiffness matrix for the specially orthotropic plane rectangular finite element has the form:

$$\begin{bmatrix} B1 & & & & & & & \\ B2 & B6 & & & & & & \\ B3 & -B4 & B1 & & & & & \\ B4 & B7 & -B2 & B6 & & & \text{Symmetric} & \\ -\frac{B1}{2} & -B2 & B5 & -B4 & B1 & & & \\ -B2 & -\frac{B6}{2} & B4 & B8 & B2 & B6 & & \\ B5 & B4 & -\frac{B1}{2} & B2 & B3 & -B4 & B1 & \\ -B4 & B8 & B2 & -\frac{B6}{2} & B4 & B7 & -B2 & B6 \end{bmatrix}$$

where the expressions B1, B2, B3, B4, B5, B6, B7 and B8 are given by:

$$B1 = \frac{t}{3}\left(\frac{E_{xx}}{r\lambda} + r\,G_{xz}\right) \qquad B5 = \frac{t}{6}\left(\frac{E_{xx}}{r\lambda} - 2r\,G_{xz}\right)$$

$$B2 = \frac{t}{4}\left(\frac{\nu_{zx}E_{xx}}{\lambda} + G_{xz}\right) \qquad B6 = \frac{t}{3}\left(\frac{rE_{zz}}{\lambda} + \frac{G_{xz}}{r}\right)$$

$$B3 = \frac{t}{6}\left(\frac{-2E_{xx}}{r\lambda} + r\,G_{xz}\right) \qquad B7 = \frac{t}{6}\left(\frac{rE_{zz}}{\lambda} - \frac{2G_{xz}}{r}\right)$$

$$B4 = \frac{t}{4}\left(\frac{\nu_{zx}E_{xx}}{\lambda} - G_{xz}\right) \qquad B8 = \frac{t}{6}\left(\frac{-2rE_{zz}}{\lambda} + \frac{G_{xz}}{r}\right)$$

Where E_{xx}, E_{zz}, ν_{zx} and G_{xz} are the equivalent elastic constants of the orthotropic medium, $r = \frac{a}{b}$ is the aspect ratio of the rectangle used, and $\lambda = (1-\nu_{xz}\nu_{zx})$. For more details on the derivation of the [K] matrix, refer to Appendix B [7].

2.3.2 METHOD OF ANALYSIS

Having established the element stiffness matrices of the individual basic elements to be used in the analysis of the sandwich panel, the next step is to assemble them to form a global stiffness matrix for the complete structures. Since the element stiffness matrices are derived with respect to the selected local coordinates which are the same as the global coordinates, no transformations are needed to obtain the stiffness relative to the global or structural coordinate system. Structure stiffness matrix can be generated by direct superposition. This is done by simple summation of the individual element stiffness coefficients for common degrees of freedom at any node. This approach to the generation of the global stiffness matrix is often referred to as the direct stiffness method.

By the direct stiffness method, a set of simultaneous linear algebraic equations will be obtained, relating loads to displacement through the structural matrix. To account for the

support conditions and prevent rigid body motion, appropriate boundary conditions must be imposed before any solution is attempted.

Once the structure stiffness matrix is obtained and boundary conditions imposed, the modified equation set must be solved for the unknown displacements. The most widely used direct method is Gaussian elimination, the main features being a forward elimination of unknowns to obtain a triangular coefficient matrix, after which the unknowns are obtained by back-substitution starting with the last modified equation.

2.3.3 COMPUTER PROGRAM

Based on the method of analysis, previously described, Fig. (2.17) shows the flow chart of a computer program which has been written to evaluate the normal stress in skin and shear stress in glue line of a sandwich panel based on the finite element method. Due to the symmetry in applied loads and panel shape, only a quarter of the whole sandwich panel has been analysed, thicker lines part in Fig. (2.18). Fig. (2.19) and (2.20) show the sandwich panel idealization and the boundary conditions. The program output is represented in Fig. (2.21) and (2.22).

CHAPTER III

EXPERIMENTAL ANALYSIS OF THERMAL STRESSES IN SANDWICH PANEL

An experimental program has been conducted to verify the mathematical analysis of thermal stresses in sandwich panels (Chapter II). The experimental work is divided into two parts, part I contains designing of what is called the 'Hot-box' (HB), preparing test specimens, and the experimental procedures. Part II contains determination of some of the elastic constants of the materials which are used as sandwich components.

PART I

3.1 THE GUARDED HOT BOX

The guarded hot box (HB) is a heat chamber used to cause gradient temperatures across a sandwich specimen. It consists of two parts, one used to increase the temperature relative to the ambient temperature (the heating box), and the second to decrease it (the refrigerator).

To construct the HB, available sandwich panels were used, each 24 x 48 x 3 in., consisting of white painted 0.024 inch aluminium on each side, a 2 x 3 inch red pine wood used as a perimeter frame, a styrofoam core, and four locks to fasten the panels to each other Fig. (3.1).

3.1.1 THE HEATING BOX

The heating box is composed of two sub-boxes, one of which stands on aluminium angles inside the other Fig. (3.2). The purpose of the guard box, which is the outer one (4 x 4 x 8 ft), is to maintain the temperatures the same as inside the metering box, which is the inner one (3 x 2 x 6 ft). The heating box is fixed on a 4 x 4 ft. platform which in turn is fixed on four casters. To prevent heat loss from the HB to the ambient room air, all the connecting joints between the elemental box panels are sealed using Latex Caulk. A secondary heater of 2000 watts (4 branches each of 500 watts, connected in a series Fig. (3.3)) is fixed on the centre line of the guard box backside at 6 inches from its bottom Fig. (3.4). An asbestos board held to the box back, behind this heater, to protect it against the high temperature. The following elements are attached to the heating box:- an electrical switch unit on the guard box backside Fig. (3.5), two thermostats on the left side, each with 25/225°F range, are to control the temperatures inside the boxes, Fig. (3.6); a fan on the guard box ceiling with a steel shaft extending between the metering box and the ceiling, on this shaft, two aluminium blades are fixed, both the same size and running clockwise, and .125 x 6 in. brown natural rubber strips fastened along the boxes free edges, by staples pressed under pressure of 100 psi using air-gun Fig. (3.7).

The metering box consists of a tubular shield, 8 x 8 x 72 in., .125 in. thick, polished inner and outer skins, ends by two 36 x 24 x .125 in. horizontal metal sheets, Fig. (3.8). A baffle panel

36 x 72 x .125 in., screwed to the two horizontal sheets as for box panel, Fig. (3.2). A primary heater of 2000 watts (4 branches each 500 watts connected in series) is fixed inside the tubular shield near its bottom end. To protect the metering box ceiling against high temperature, an asbestos board is glued to it using contact cement.

3.1.2 WARM AIR CIRCULATION

The thermostats dials are set to the temperature desired, the temperatures inside the boxes increase, the fan pulls the warm air up inside the tubular shield and down in front of the baffle sheet, circulating the warm air continuously. When the temperatures inside the boxes reach the setting of the thermostats, the heating is interupted. Since heat is lost to ambient air as well as to the cooling box, the circulating air temperature decreases. This is sensed by the sensitive thermostats bulbs and heating is restarted. A fluctutation of 5°F is noticed while cycling about final temperature value.

3.1.3 REFRIGERATOR

The refrigerator half of the box is 2 x 4 x 8 ft. The refrigeration system consists of condensing and refrigerating units. The condensing unit is fixed to a 2 x 4 ft. stand attached to the back side of the box, Figs. (3.9) and (3.10). The refrigerating unit is composed of cooling coil fixed between two vertical, .125 x 48 x 60 in. aluminium inner and outer skins. Two horizontal, .125 x

20 X 48 in. metal sheets screwed to these two vertical sheets, one 6 in. from the refrigerator ceiling and the other 30 in. from its bottom, Figs. (3.11) and (3.12). A baffle plate .125 x 48 x 8 in. screwed to the two horizontal sheets, as for box panel. A water drain is tilted on the box bottom. The refrigerator box is furnished with the following elements: a thermostat with -25/100°F range, fixed on the box back side, a fan to the box ceiling center inside it, and AC magnetic relay fixed on the box back side to the left.

3.2 STRAIN GAGES

The strain gages which were used to measure the thermal strains in the skins of a sandwich specimen were based on the instructions of the Intertechnology Inc. manual, which shows a straight forward method to guide in the following steps:

- strain gage selection
- the measuring circuit
- strain gage installation
- lead attachment to strain gages

3.3 PORTABLE POTENTIOMETER

To measure ambient and skin temperatures, the copper constantan thermocouples were used. A portable potentiometer, Model 2745, Fig. (3.14), used to measure the thermocouples voltages.

The steps for manual compensation of the end of the thermocouple junction Fig. (3.15) have been done according to instructions for portable precision potentiometer, Model 2745.

3.4 TEST SPECIMEN

3.4.1 SPECIMEN PREPARATION

The following procedures are followed in sandwich specimen preparation:

1 - The aluminium facings of the specimen cut from 4 x 10 ft., flat polished aluminium sheet, using snips then their edges filed.

2 - Using SNAP soap, tap cold water, these facings washed, wiped using clean, dry sponge and left for an hour in the normal air conditions.

3 - A piece of white pine wood, 2 x 4 x 36 in. (nominal), selected from among five similar pieces (it had no knots or texture defects). Its surface sanded using mechanical sander and the sawdust removed, using a dry sponge.

4 - The actual dimensions of the aluminium facings and the wood core were measured using calibre.

5 - Epoxy adhesive preparation -

The epoxy adhesive which was used was BOSTIK 7087 - it contained two liquid parts, ie, part A contains curing agents, and part B contains epoxy resin. This is mixed in equal volume into a smooth paste just prior to use.

6 - The aluminium facings fully coated with the epoxy adhesive paste and by using a clean sharp edged piece of aluminium, the coating is spread, then leveled.

7 - The wood core sandwiched between two aluminium facings, the whole specimen squeezed between two flat pieces of birch wood (each with the same dimensions as the core) clamped using six clamps, and left

48 hours for adhesive curing, Fig. (3.16).

3.4.2 STRAIN GAGES POSITIONS ON SKINS

Using the strain gages installation technique (3.2), five rosette gages, type EA-13-125RA-120, were installed on each of the specimen faces, along half the length, in addition to them, another four single gages type EA-13-125BT-120 were installed near the specimen end on one face only. The positions of the gages are shown in Figs. (3.17) and (3.18).

3.5 TEST PROCEDURES AND RESULTS

3.5.1 INSTRUMENTATION

1 - The hot box (3.1)

2 - Portable potentiometer (3.3)

3 - Portable digital strian indicator, model P-350, with ten-channel switch and balance unit model SB-1, Fig. (3.19).

4 - A sandwich plate, 8 x 6 ft, composed of six 2 x 4 ft. sandwich panels, mentioned earlier. A 36 x 4 in. opening centered this plate with one in. thick sponge strip fixed along its edges. In this opening the sandwich specimen is inserted. To decrease heat loss between the two parts of the HB, fiberglass insulation is taped to the plate facings, Fig. (3.20).

3.5.2 TEST PROCEDURES

1 - The sandwich plate, with the specimen inserted in its opening, is held between the refrigerator and the heating boxes. The HB locked properly such that it is isolated from the ambient, Fig. (3.21).

2 - The free ends of thermocouples connected to a switch unit and the emf of all thermocouples junctions compensated (3.3). The dials of the thermostats set to the temperatures at which stop is desired. The initial readings of all the thermocouples taken and recorded.

3 - The leadwires of the strain gages connected to the binding posts on the switch unit.

- the appropriate gage leads connected from the switch unit to the binding posts on the strain indicator, following the strain indicator instructions for completing the wheatstone bridge with the 120-ohm dummy gage.

- the gage factor control on the strain indicator set to the value given on the information sheet in the strain package.

- the strain indicator turned ON, its measuring dial set to zero and the meter needle brought to the null position with the gage balance control on the switch unit (this step has done for each strain gage, and in case the meter needle cannot be brought to the null position, the measuring dial set to initial value and the meter needle brought to the null using the balance control. In this case, the initial value was the zero reading for the concerned gage). The initial readings for all the strain gages are recorded. NOTE that steps 2 and 3 are done simultaneously.

4 - the electrical switch unit on the back side of the HB was turned ON.

5 - the thermostat setting was reached after about one hour. To ensure reaching a stable temperature, the readings of the strain

indicators and the potentiometer started after another hour when there was less than 0.02 millivolt change in the potentiometer reading each five minutes (all the readings have been taken simultaneously and then recorded).

6 - the thermostats dials were set to the next desired temperatures and the whole procedure repeated again.

7 - at the end of this test, the refrigerator and heating boxes were separated and the panel allowed to cool.

8 - when the sandwich specimen come back to its normal conditions, after two days, the sandwich plate, with the specimen, turned about and the test procedures repeated again.

3.5.3 TEST RESULTS

The normal stresses are calculated from the measured thermal strains and the results are presented on curves in Figs. (3.22) to (3.26).

PART II

The sandwich specimen, which is used in this experimental programme is composed of two aluminium facings and a white pine wood core. The following are experimental procedures which are followed to determine some of the elastic constants for those materials.

3.6 MATERIAL PROPERTIES

See Appendix C

CHAPTER IV

RESULTS, DISCUSSION AND CONCLUSION

4.1 COMPARISON

A simplified formula (overall behaviour) and mathematical solution for the normal stress in the skin are given. The results of both approaches are in agreement at the centre line of the skin and this is considered as the first check on the mathematical analysis.

The summation of Fourier series, which appear in the normal and shear stress formulas, are checked by comparing the summation computed values from the mathematical solution. Both values are shown on the curves in Fig. (2.11), (2.12) and the results are seen to be exactly the same (Fig. 2.14, 2.15).

For the case of uniform temperature change a comparison is made between the mathematical and the finite element results. There is a difference less than 6% of the mathematical value at the skin centre line and this is considered as a second check on the mathematical analysis. The actual comparison being shown on Fig. (4.6) and (4.7).

The experimental and the mathematical results are compared. There is good agreement between the normal stress component due to the gradient temperature change while there is a difference up to 300 psi in the stress component due to the uniform temperature change. The shear rigidity effect on the modulus of elasticity of the wood is very small and the differences may be due to the following causes:

- The strain indicators null balancing process caused an error ±40μ strain (400 psi) due to doing it manually.
- The installation and soldering process of the strain gages affect the output.
- The strain indicator zero shift.
- Nonhomogenuity of the core, influence of glue line and the assumed expansion coefficient of the wood.

4.2 CONCLUSION

1 - Formulas have been developed for the normal and shear stresses in skins and glue lines respectively of flat faced sandwich panels due to uniform and gradient temperature changes.

2 - Formulas have been presented for predicting the deflections of sandwich panel due to uniform and gradient temperature changes.

3 - It has been demonstrated that high shear stresses occur at the ends of the glue line. A stress of 500 psi can be created by a temperature change on one side of 80° F.

4 - The mathematical formulas have been shown to be in reasonable agreement with experimental results.

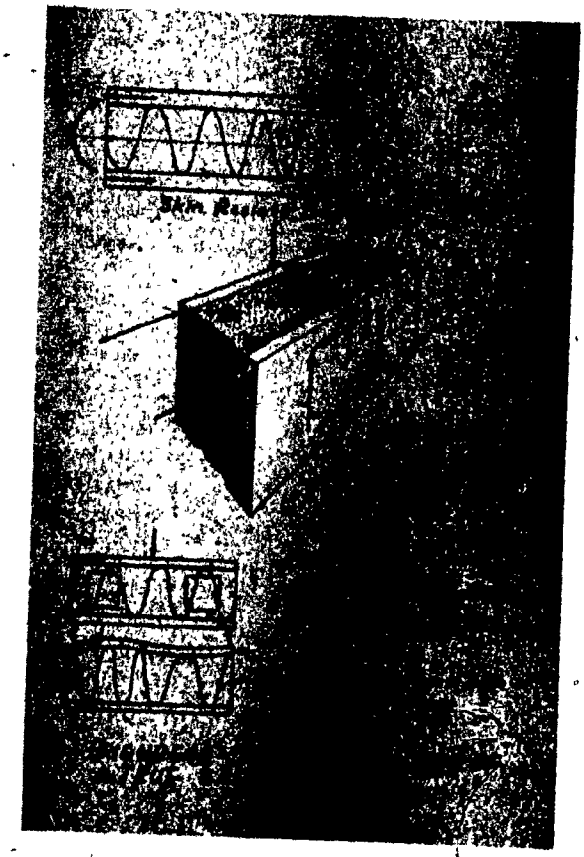

FIG. 1.1: STRUCTURAL ACTION OF A TRUE SANDWICH PANEL

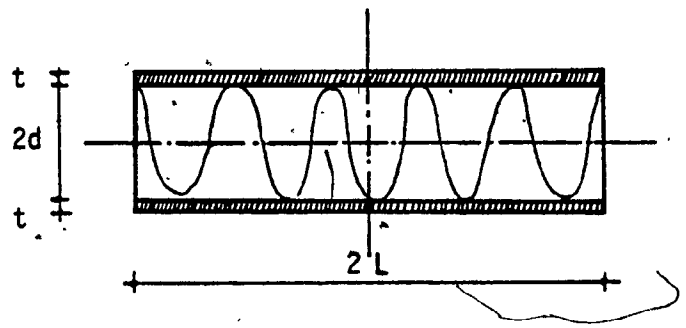

FIG. 2.1: CROSS SECTION OF SANDWICH PLATE

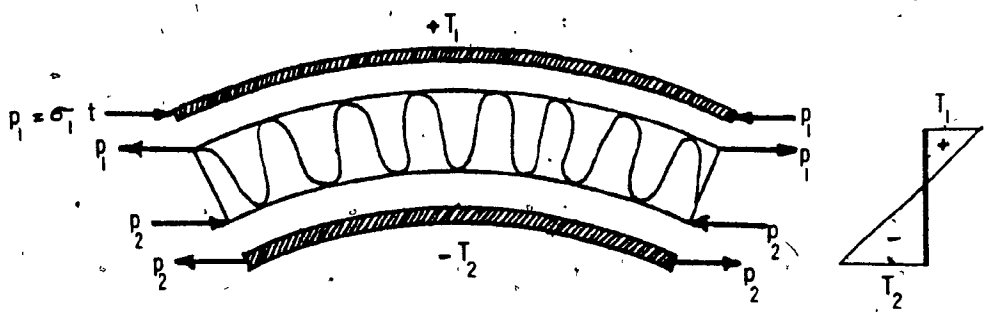

FIG. 2.2: THERMAL FORCES IN THE GLUE LINE

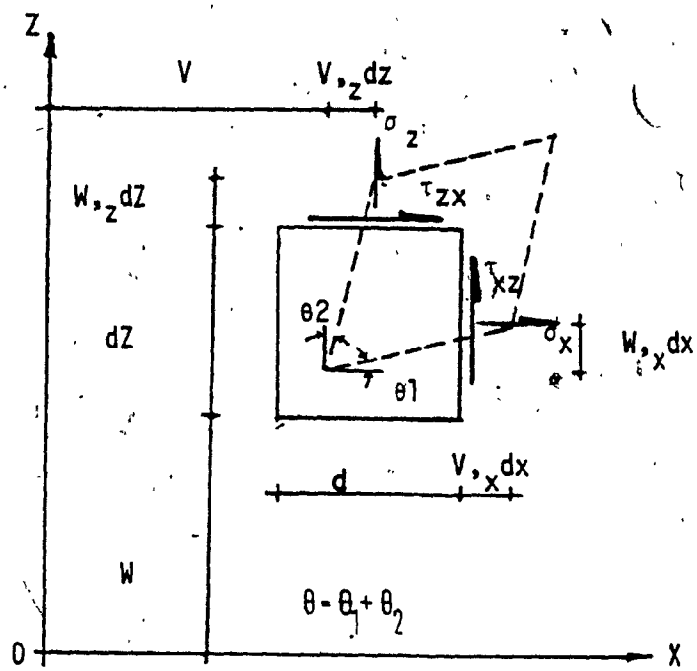

FIG. 2.3: DISPLACEMENT AND DISTORTION OF AN INFINITESIMAL ELEMENT

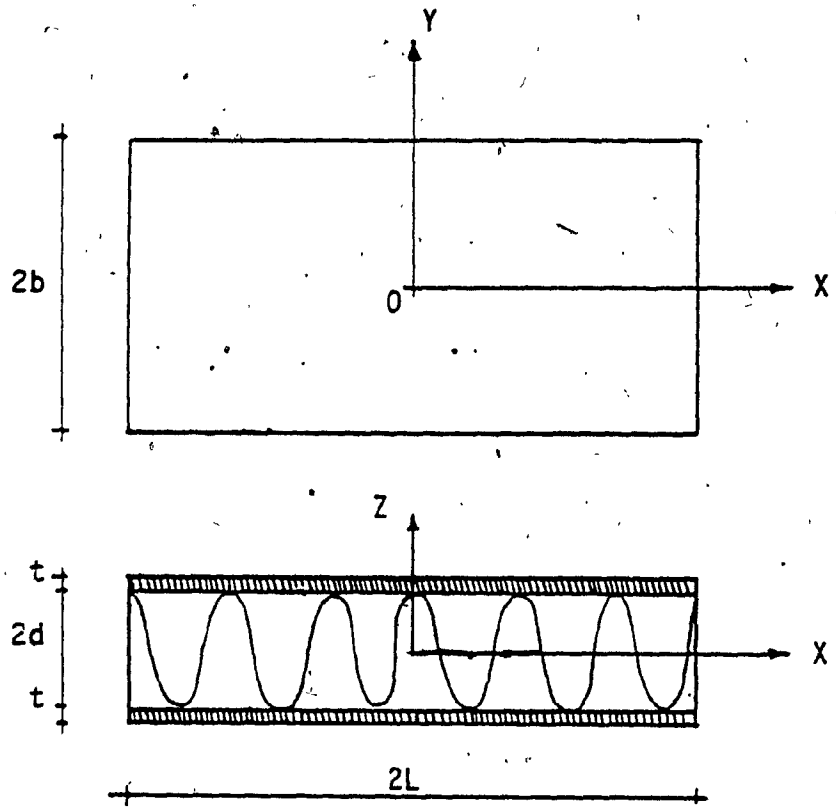

FIG. 2.4: SANDWICH PANEL DIMENSIONS

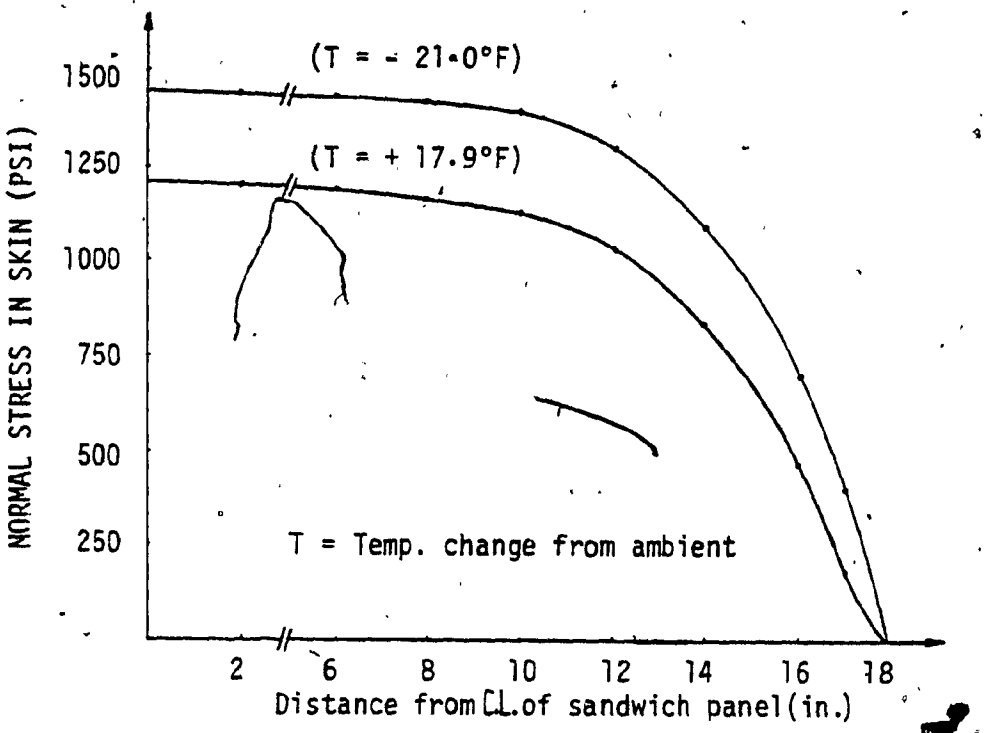

FIG. 2.5: FINAL STRESS IN SKIN
(based on theory of elasticity)

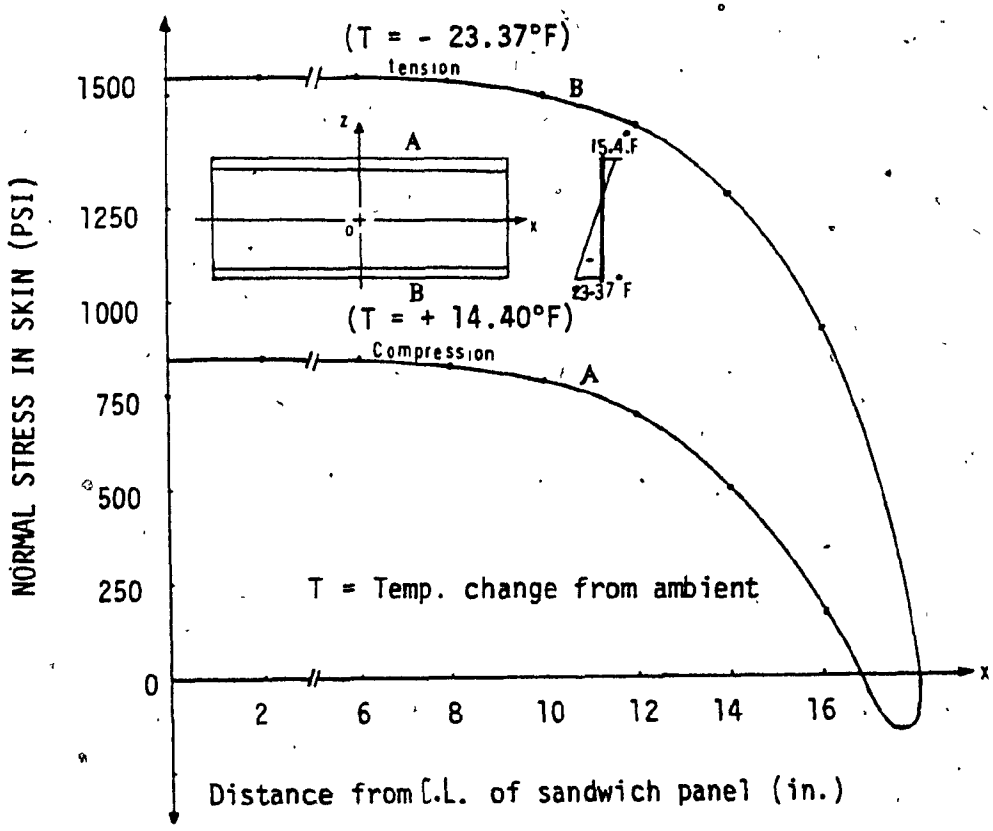

FIG.2.6 : FINAL STRESS IN SKIN

(Based on theory of elasticity)

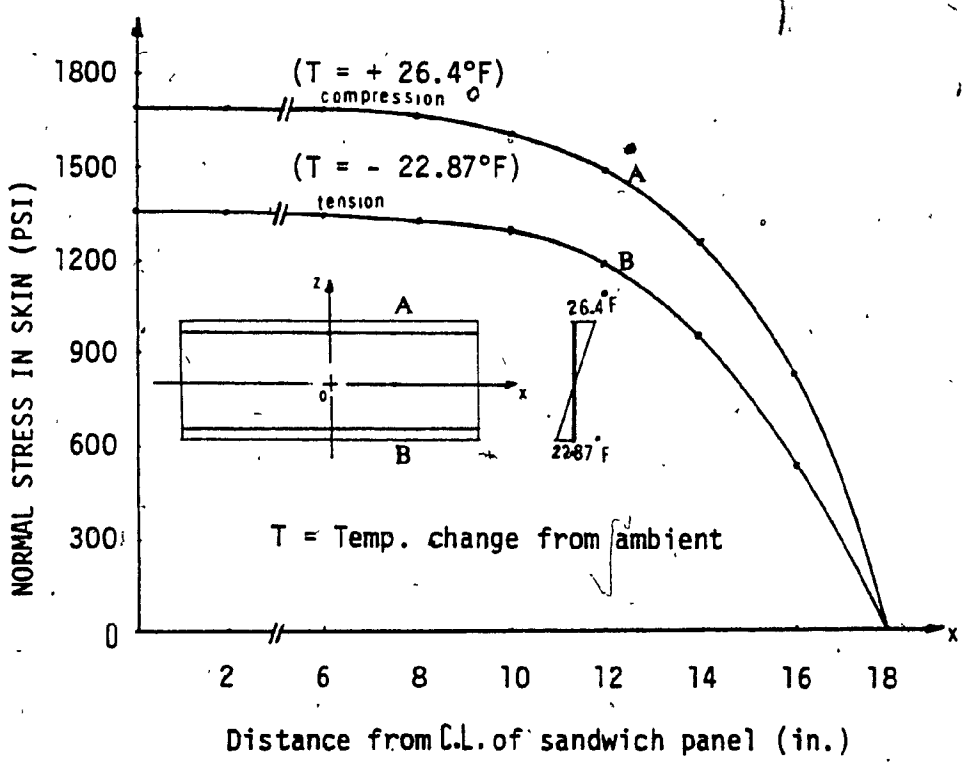

FIG. 2.7: FINAL STRESS IN SKIN
(Based on theory of elasticity)

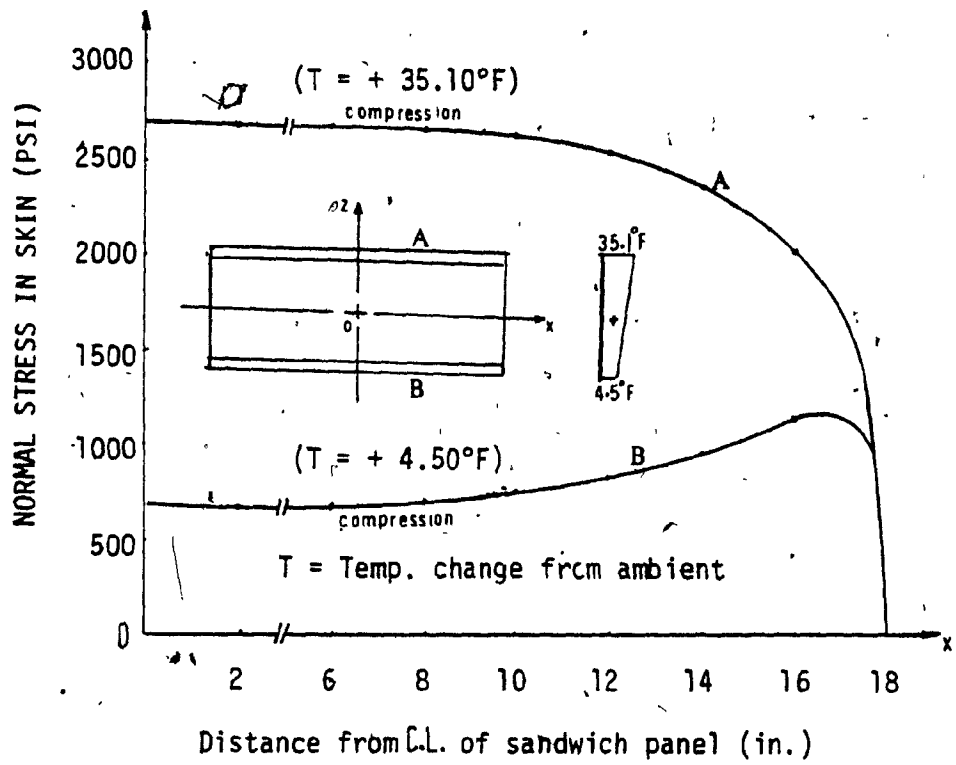

FIG. 2.8: FINAL STRESS IN SKIN
(Based on theory of elasticity)

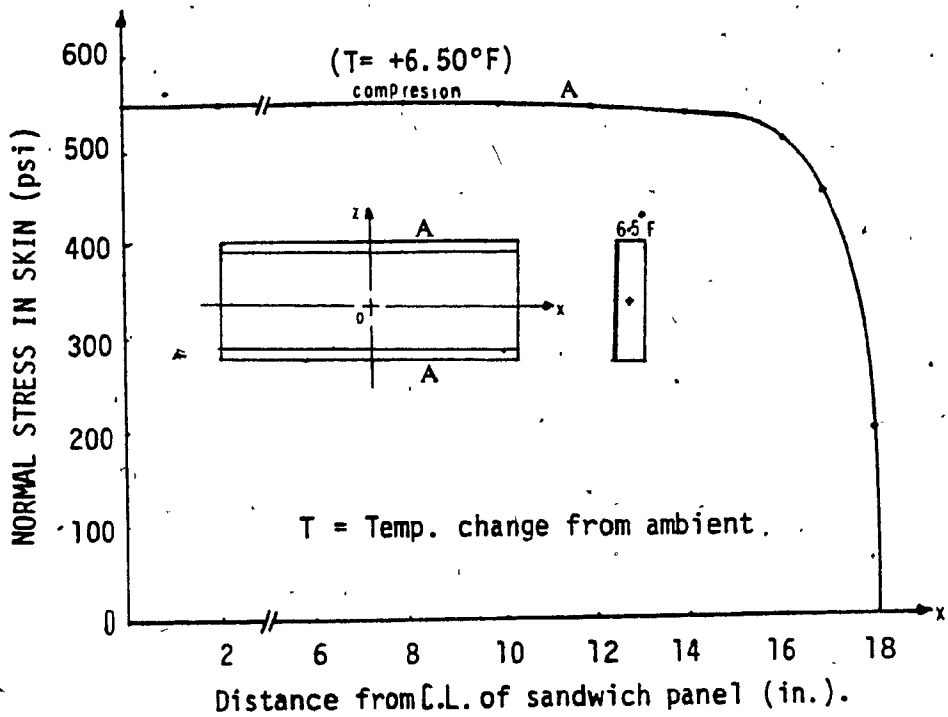

FIG. 2.9 : FINAL STRESS IN SKIN
(based on theory of elasticity)

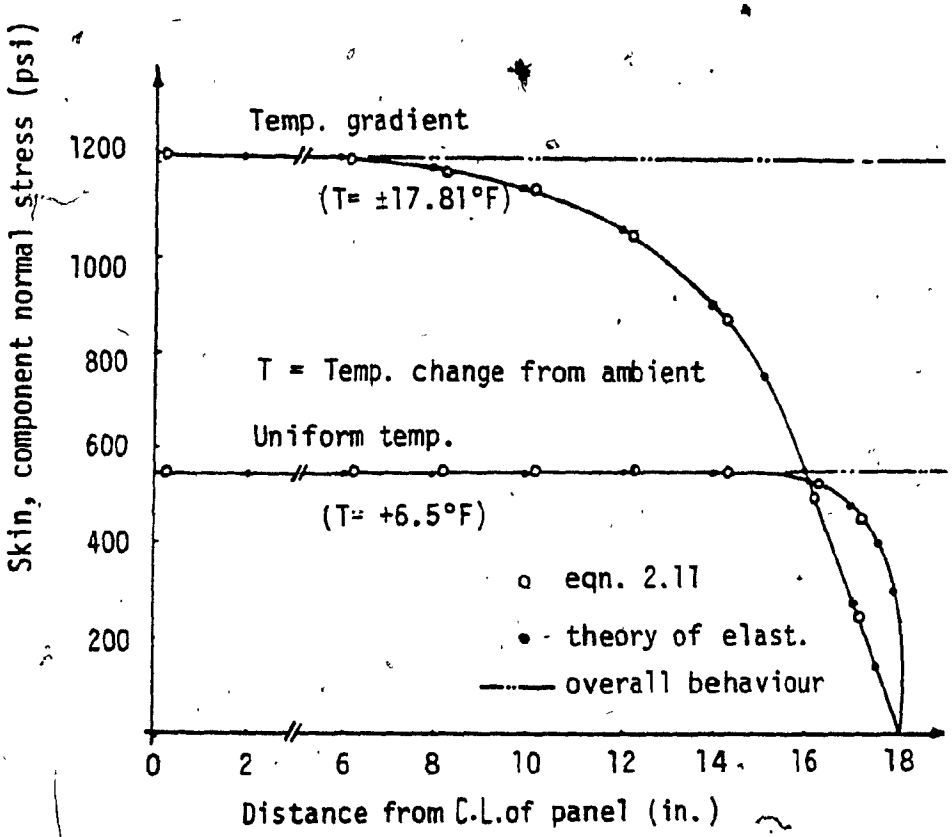

FIG. 2.10 : COMPONENT NORMAL STRESS IN SKIN
(Based on theory of elasticity)

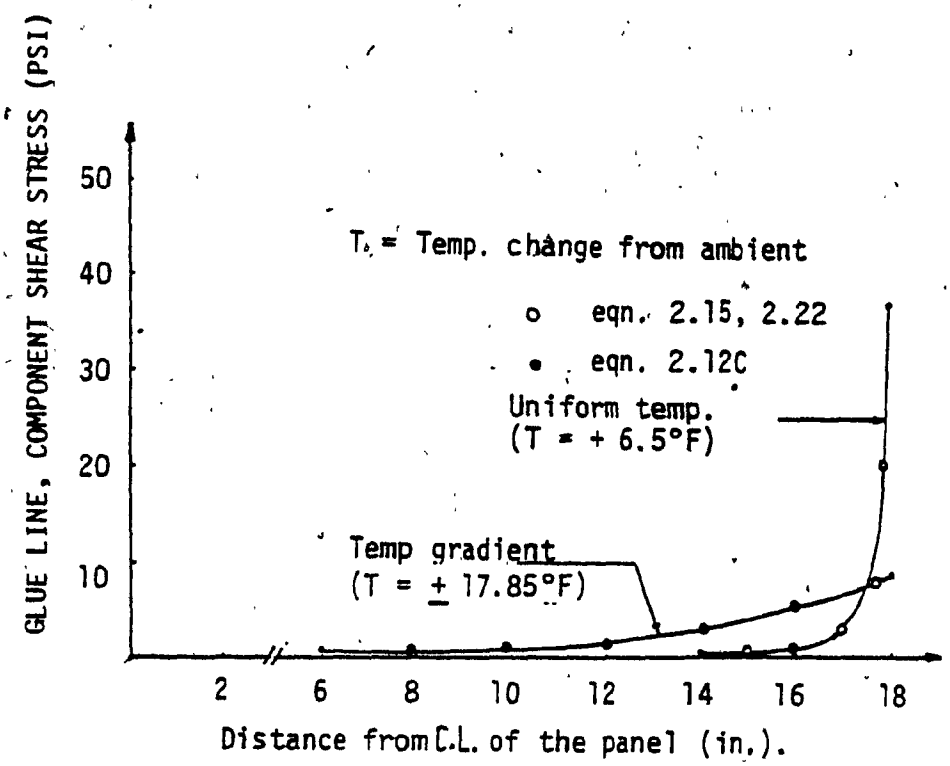

FIG. 2.11: COMPONENT SHEAR STRESS IN GLUE LINE
(Based on theory of elasticity)

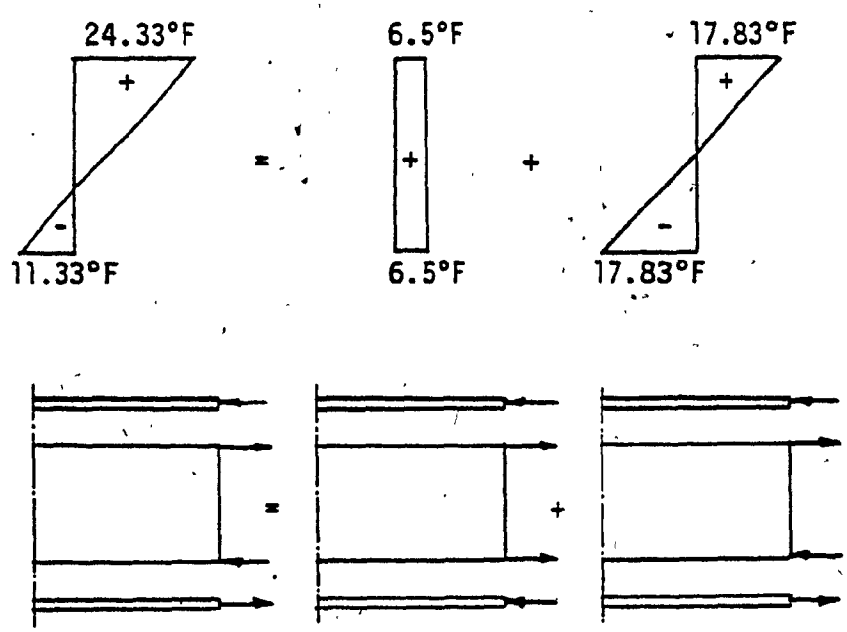

FIG. 2.12: STRESS SUPERIMPOSING

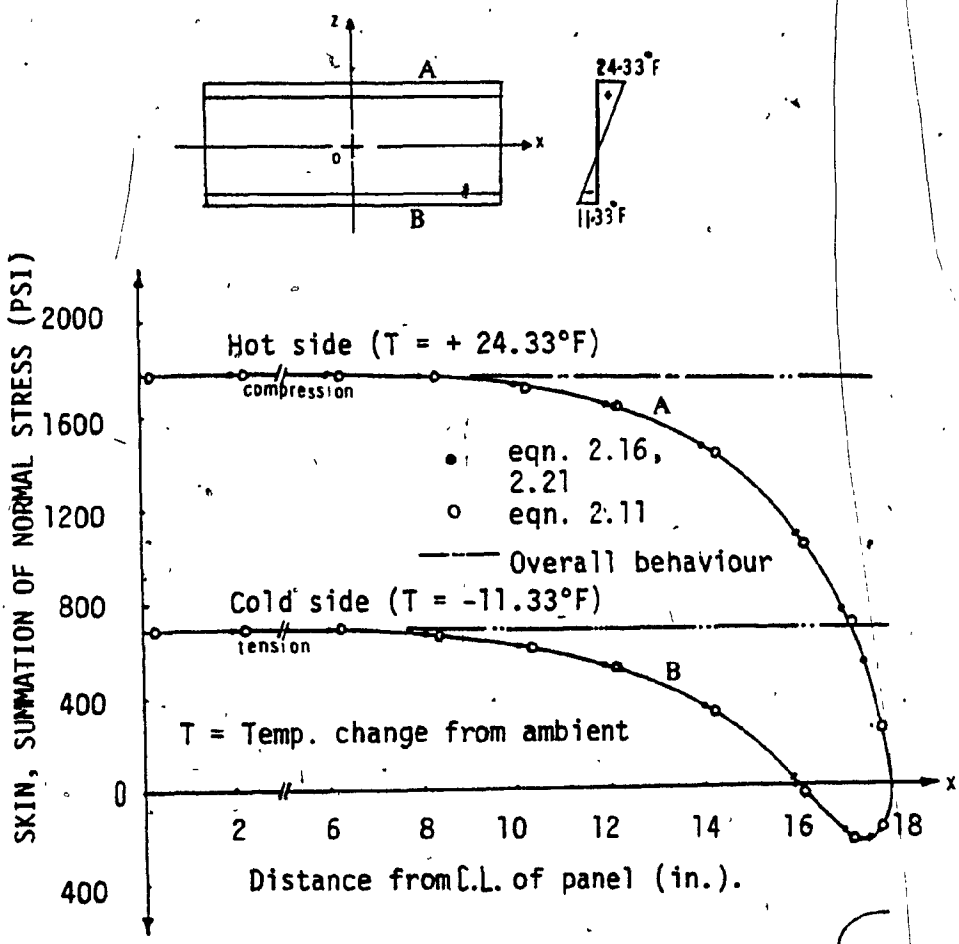

FIG. 2.13: FINAL STRESS IN SKIN
(Based on theory of elasticity)

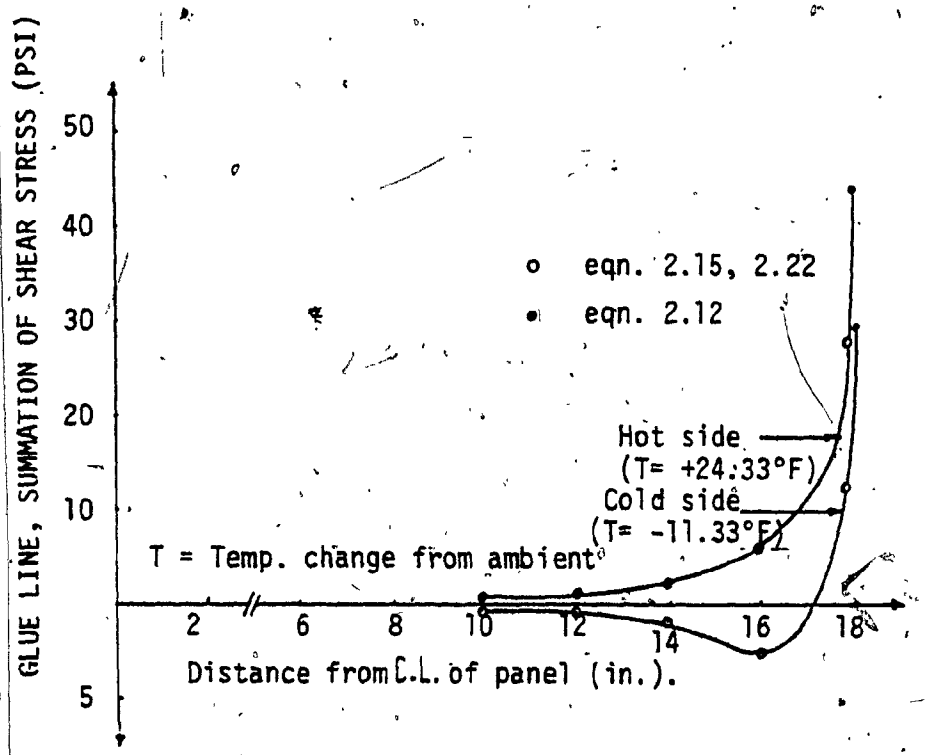

FIG. 2.14: FINAL SHEAR STRESS IN GLUE LINE
(Based on theory of elasticity)

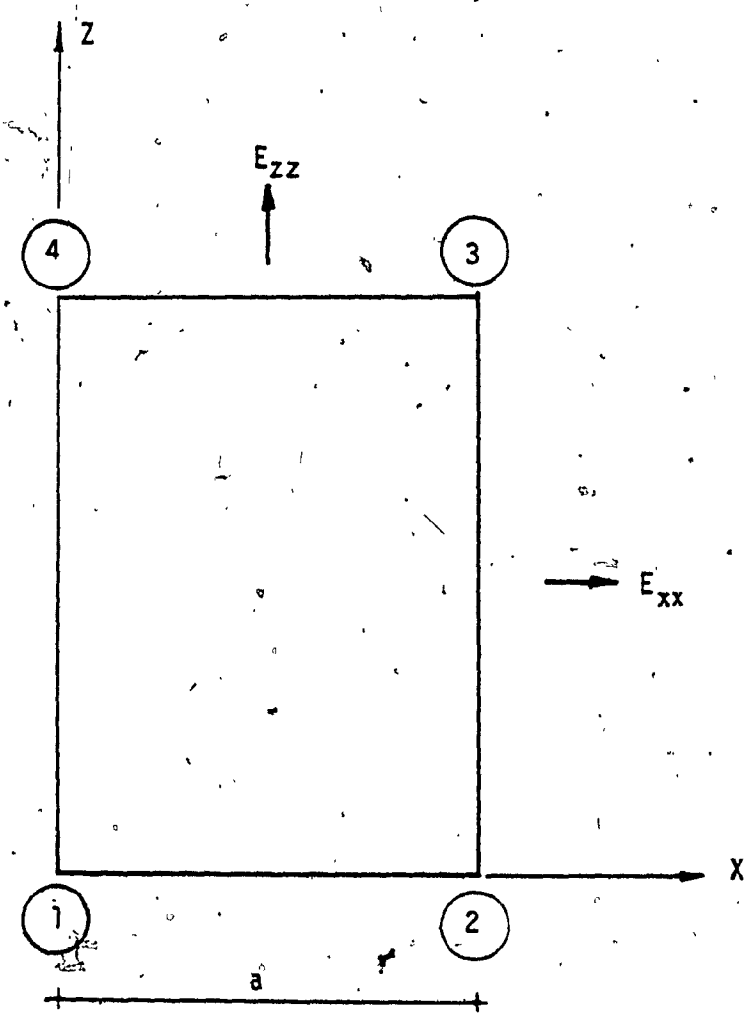

FIG. 2.15: RECTANGULAR ELEMENT USED IN MODELING THE SANDWICH PANEL.

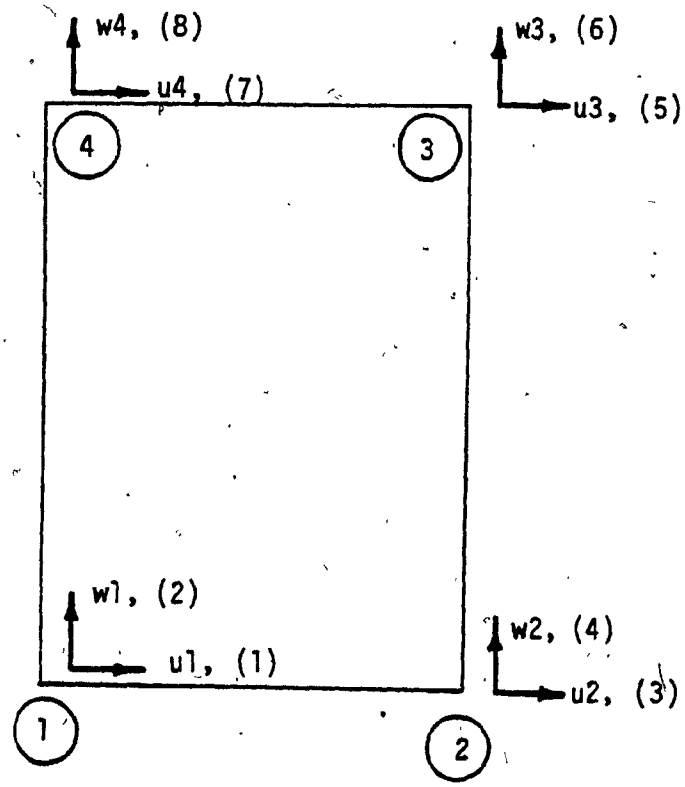

FIG.216 : DEGREES OF FREEDOM AND SEQUENTIAL NUMBERING FOR SKIN ELEMENT OR CORE ELEMENT (u is replaced by v)

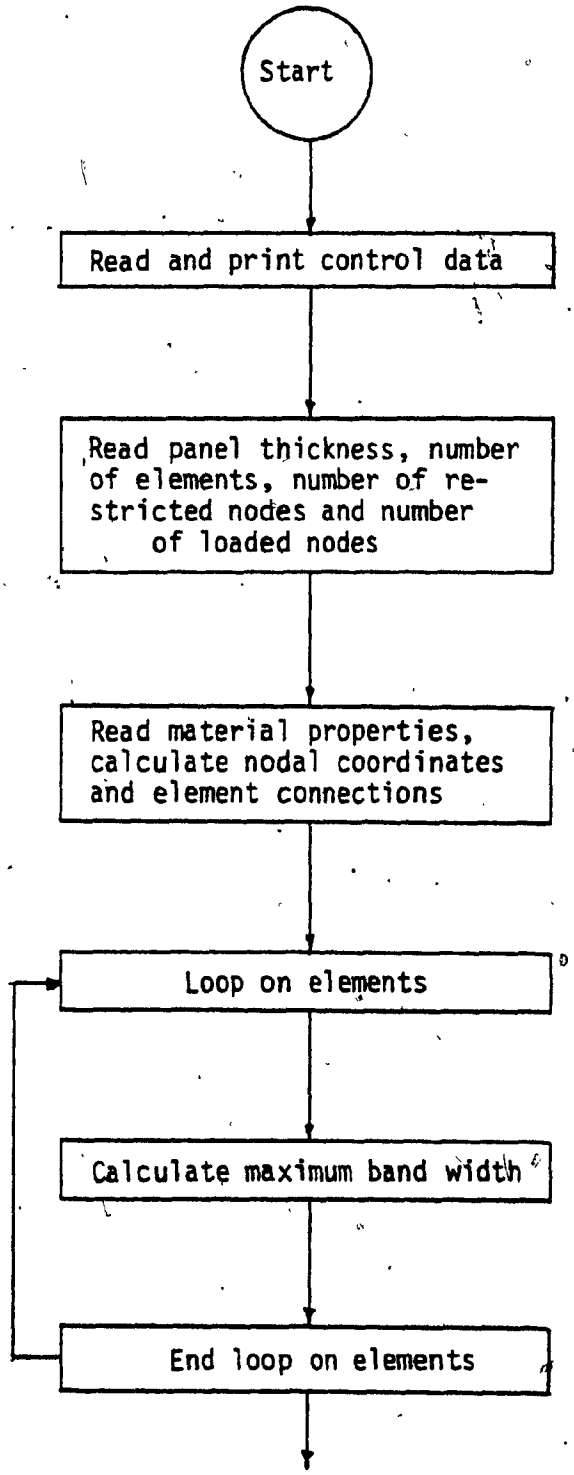
Start
Read and print control data
Read panel thickness, number of elements, number of restricted nodes and number of loaded nodes
Read material properties, calculate nodal coordinates and element connections
Loop on elements
Calculate maximum band width
End loop on elements

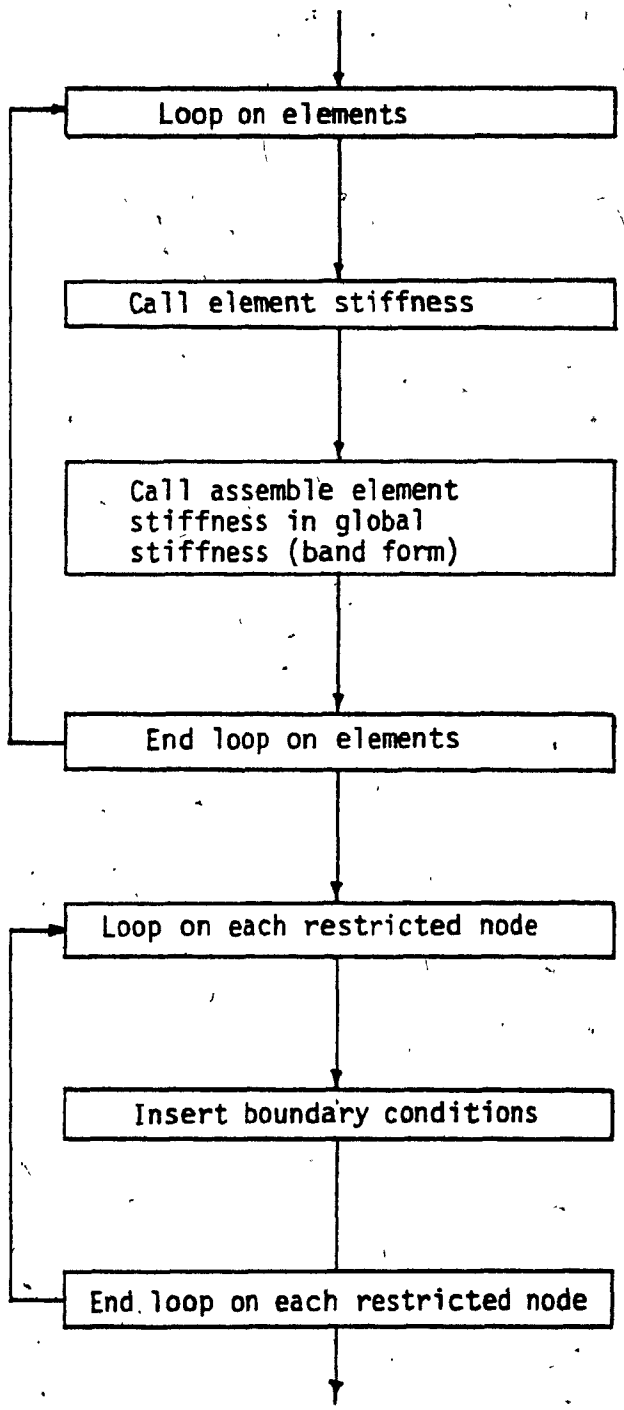
Loop on elements
Call element stiffness
Call assemble element stiffness in global stiffness (band form)
End loop on elements
Loop on each restricted node
Insert boundary conditions
End loop on each restricted node

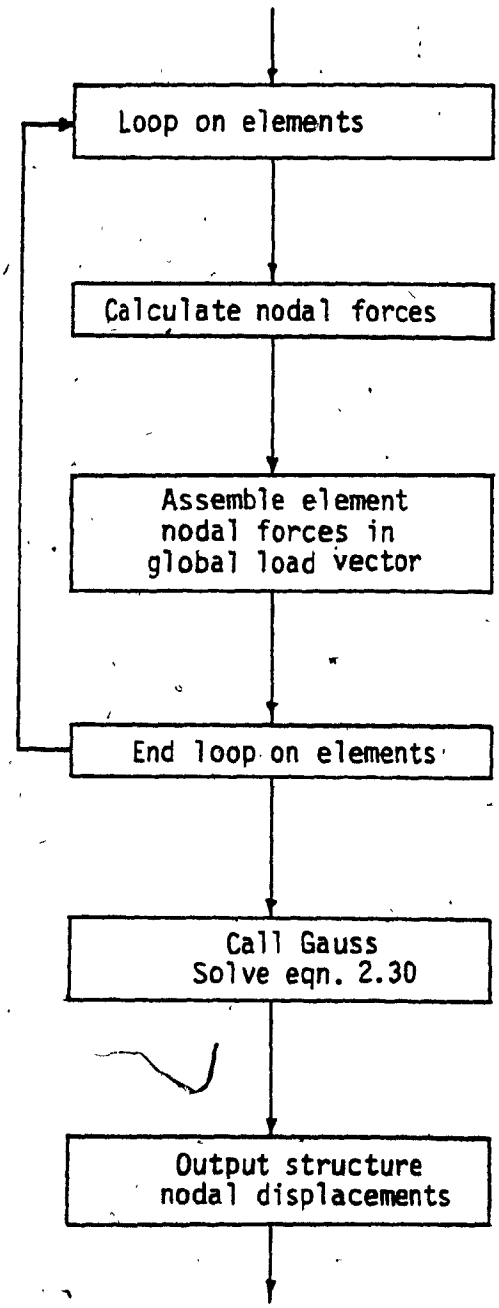
Loop on elements
Calculate nodal forces
Assemble element nodal forces in global load vector
End loop on elements
Call Gauss Solve eqn. 2.30
Output structure nodal displacements

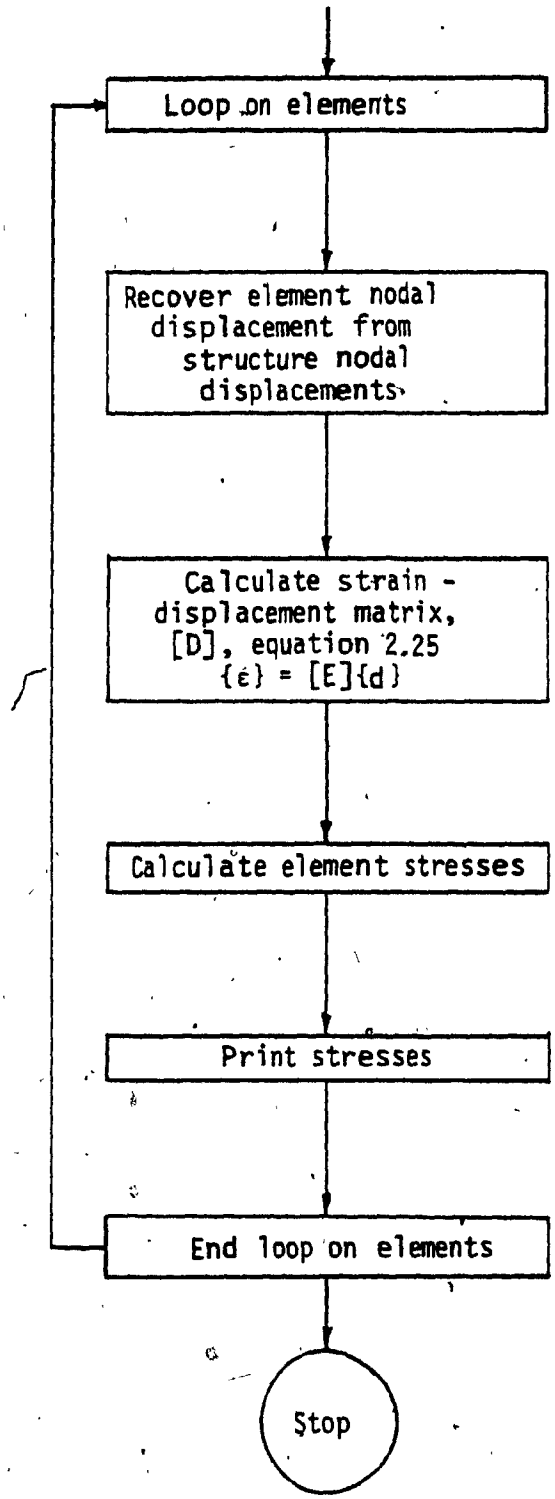

FIG. 2.17: FINITE ELEMENT COMPUTER PROGRAMME FLOW CHART

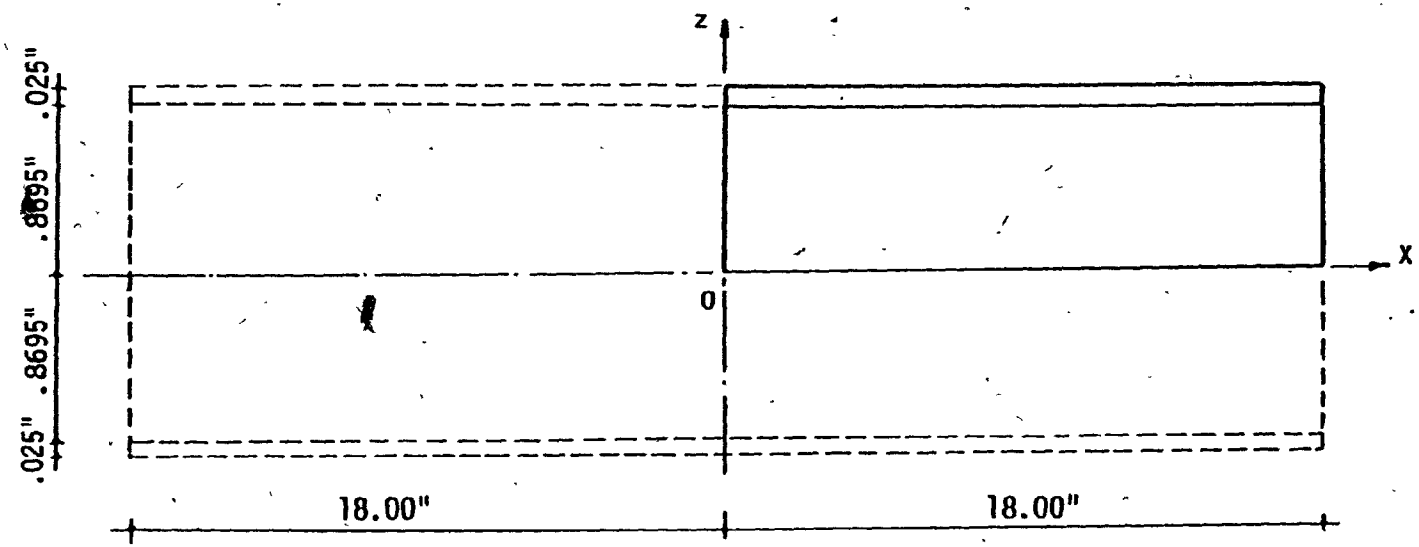

FIG. 2.18: SANDWICH PANEL
(thicker lines analysed only)

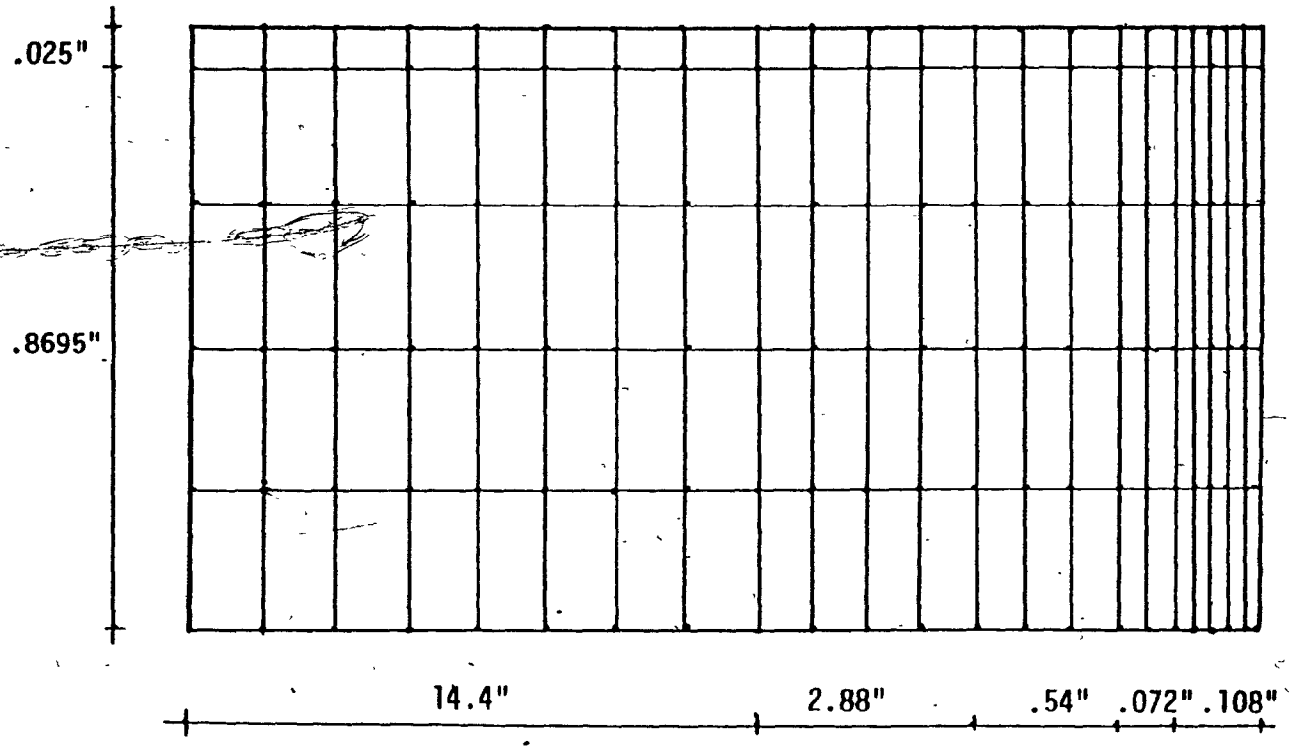

FIG. 2.19: DISCRETIZATION OF SANDWICH PANEL

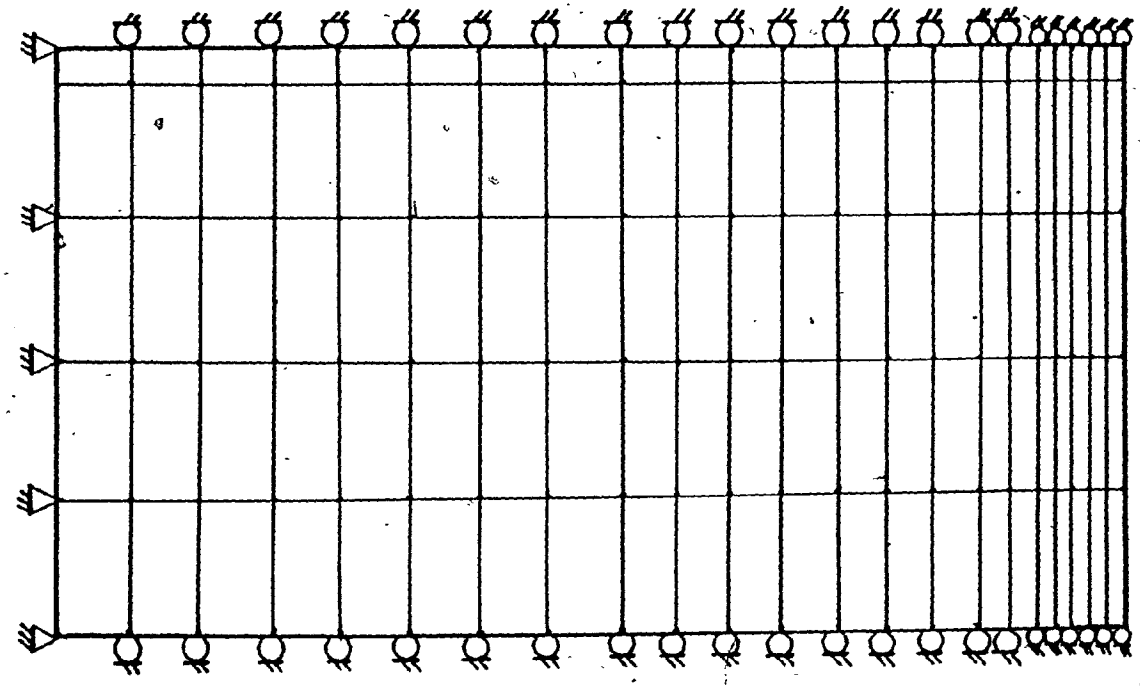

FIG. 2.20: BOUNDARY CONDITIONS FOR UNIFORM TEMPORATURE CHANGE

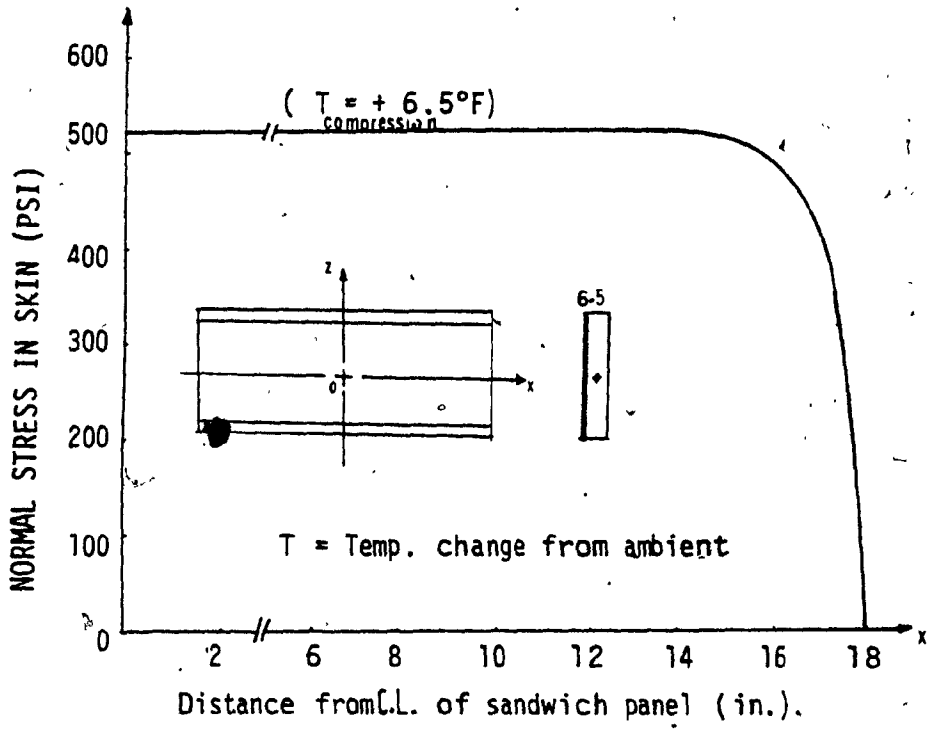

FIG. 2.21: FINAL STRESS IN SKIN
(Based on finite element method).

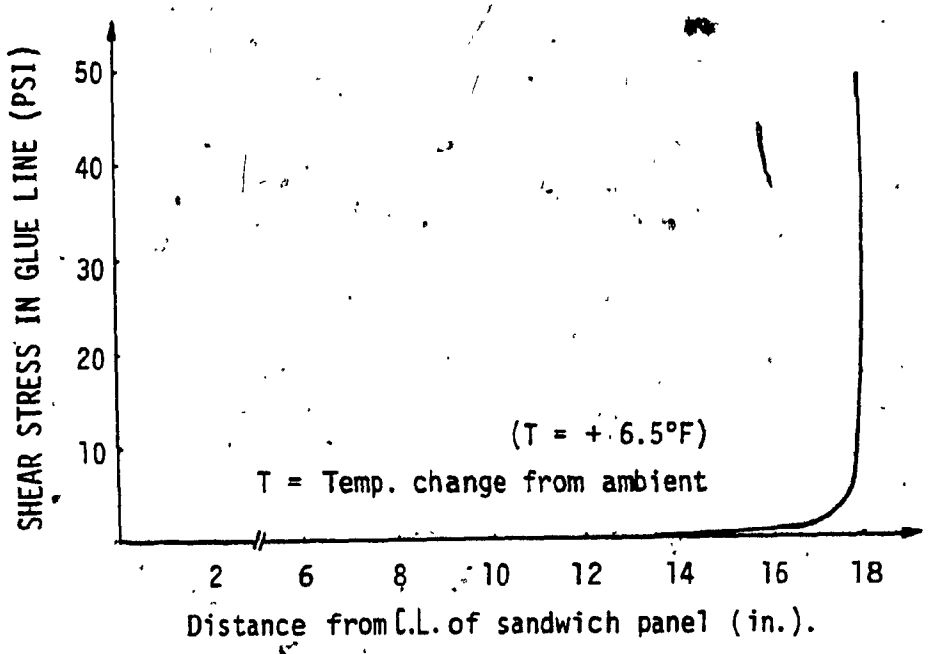

FIG. 2.22: FINAL STRESS IN GLUE LINE
(Based on finite element mehtod)

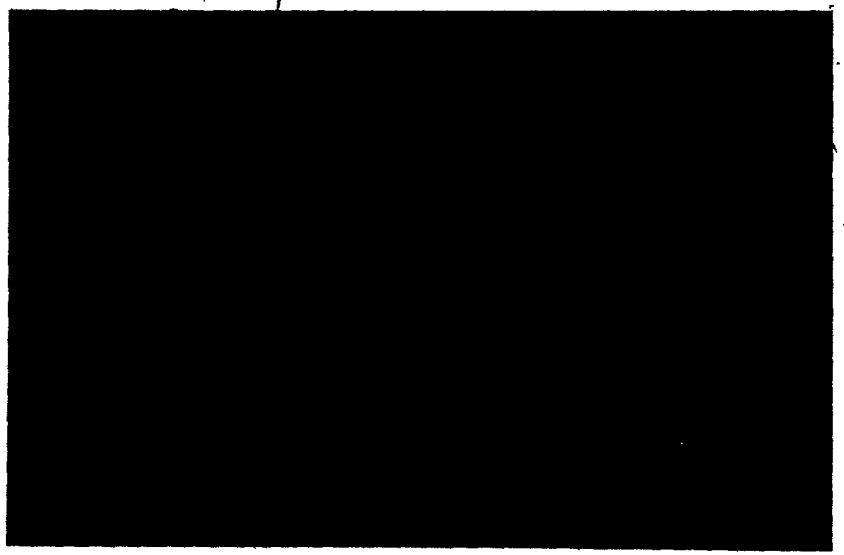

FIG. 3.1: ELEMENTAL SANDWICH PANEL OF THE HOT-BOX

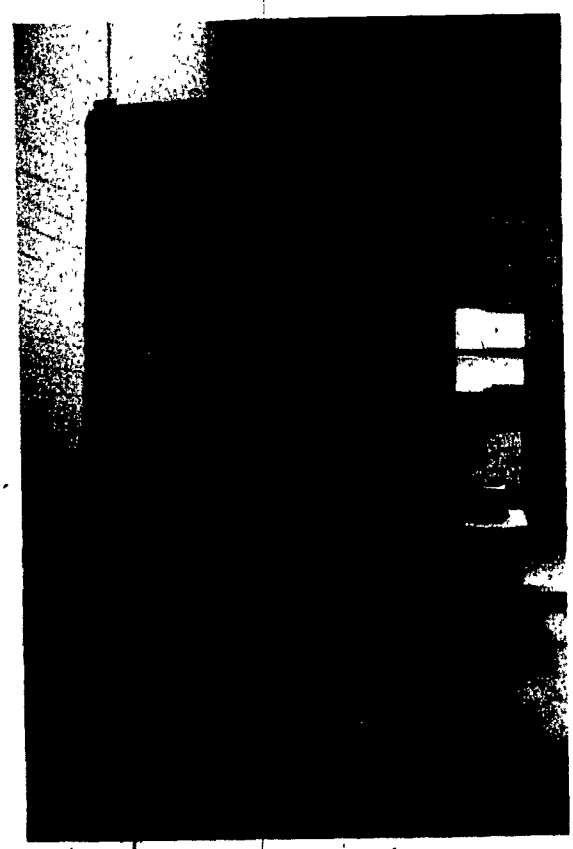

FIG. 3.2: HEATING SIDE OF THE HOT-BOX

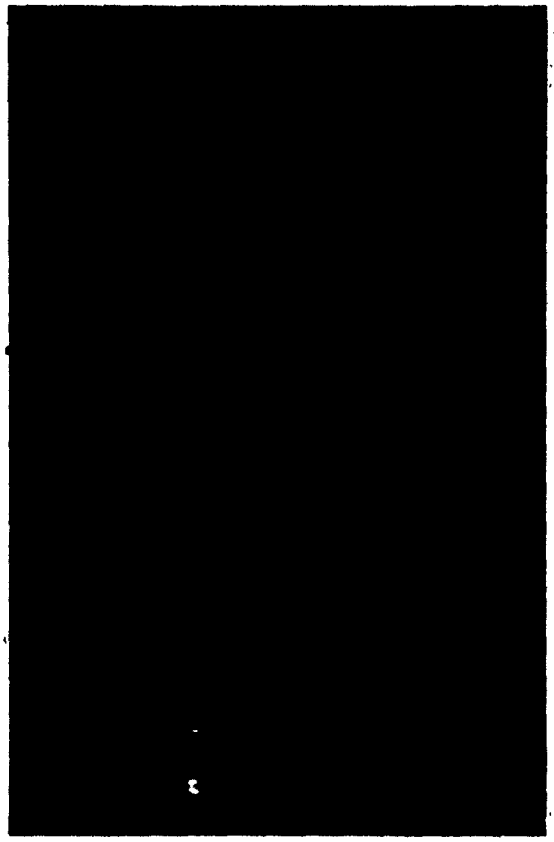

FIG. 3.3: A HEATING ELEMENT OF THE HOT-BOX

FIG. 3.4: GUARD BOX OF THE HEATING SIDE OF THE HOT-BOX

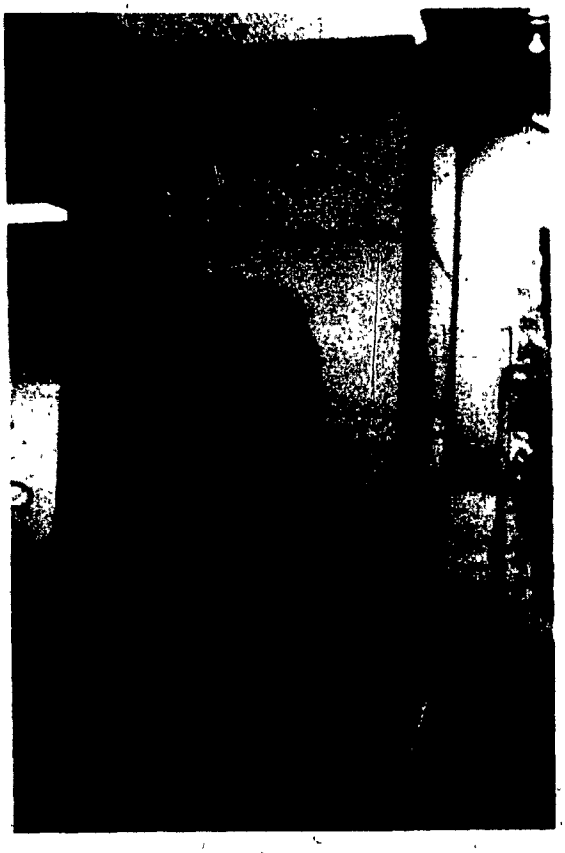

FIG. 3.5: BACK SIDE VIEW
OF THE GUARD BOX

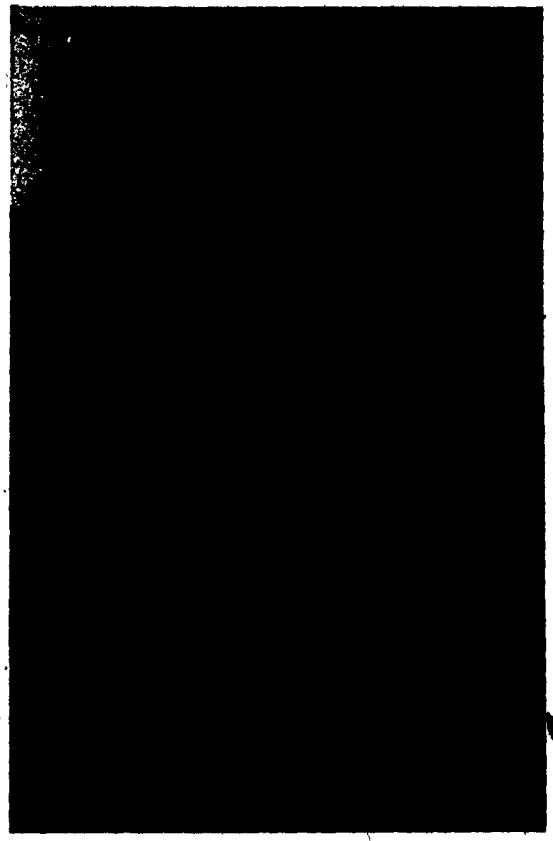

FIG. 3.6: LEFT SIDE VIEW OF THE GUARD BOX

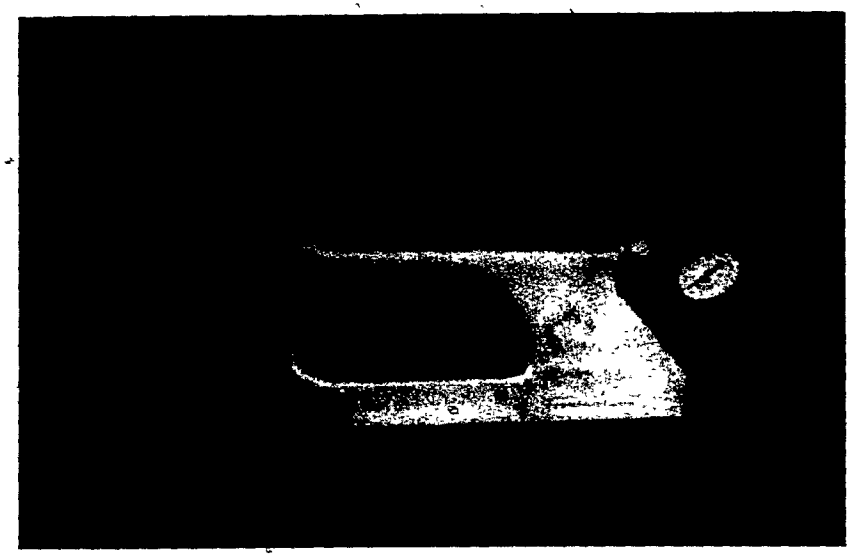

FIG. 3.7: AIR-GUN USED IN STAPLING THE RUBBER EDGES OF THE HOT-BOX

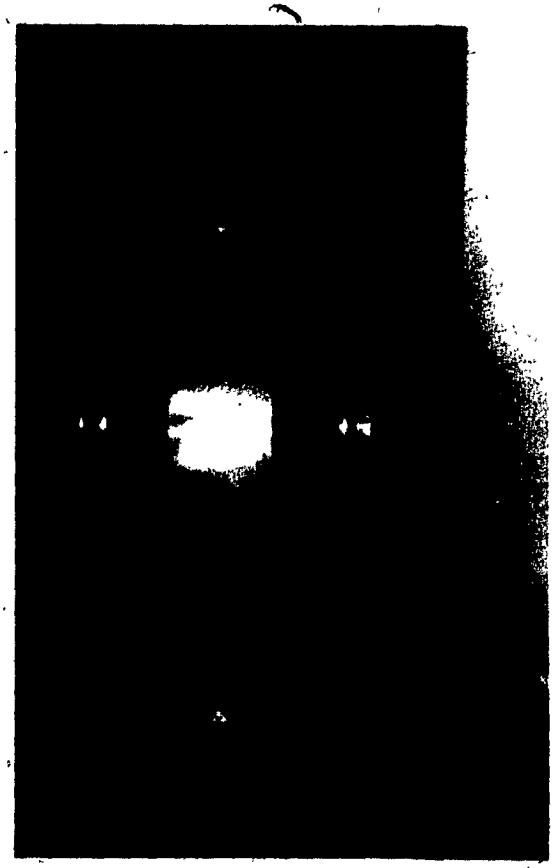

FIG. 3.8: METERING BOX OF THE HEATING SIDE OF THE HOT-BOX

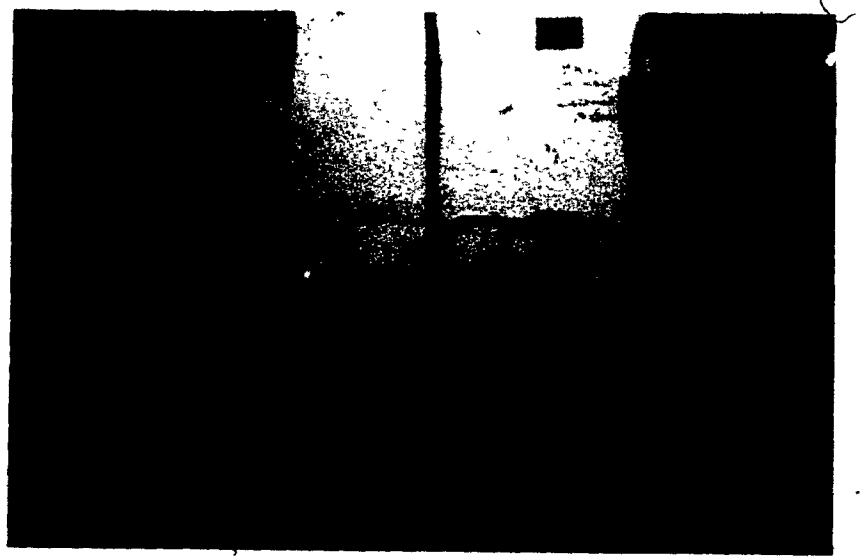

FIG. 3.9: CONDENSING UNIT OF THE REFRIGERATOR

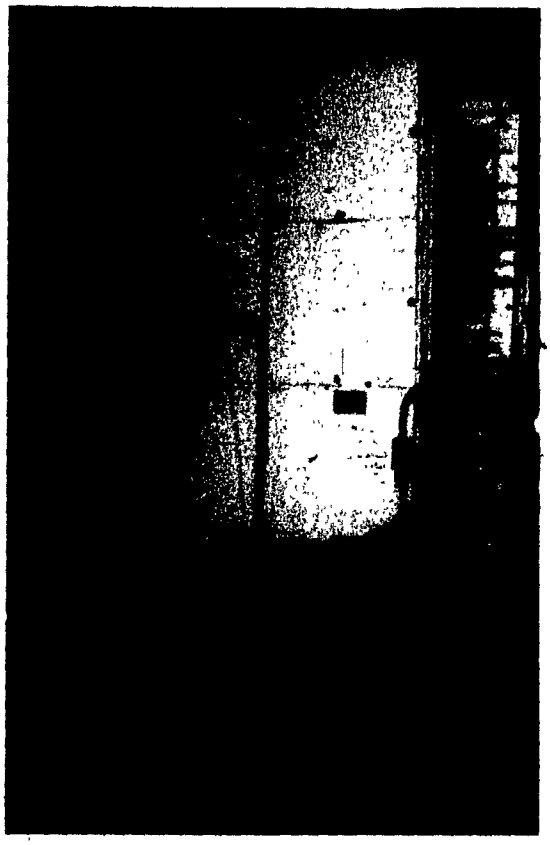

FIG. 3.10: REAR VIEW OF THE REFRIGERATOR

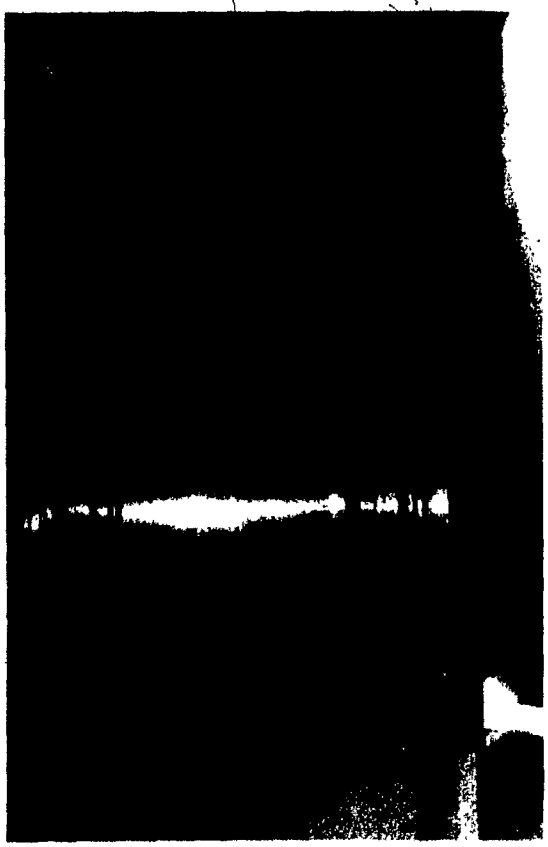

FIG. 3.11: COOLING COIL INSIDE THE REFRIGERATOR

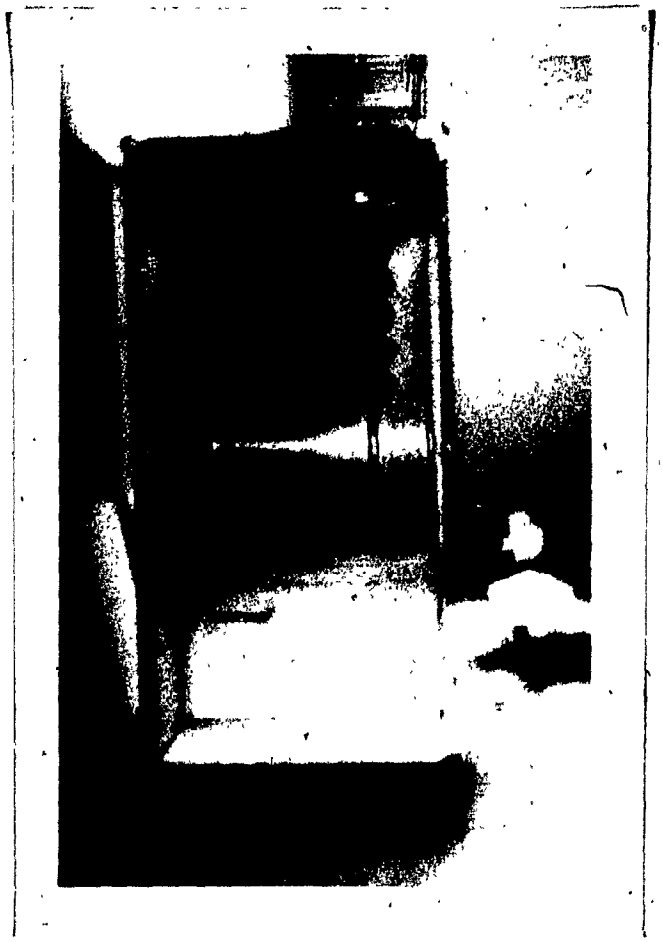

FIG. 3.12: THE REFRIGERATOR DURING ASSEMBLY

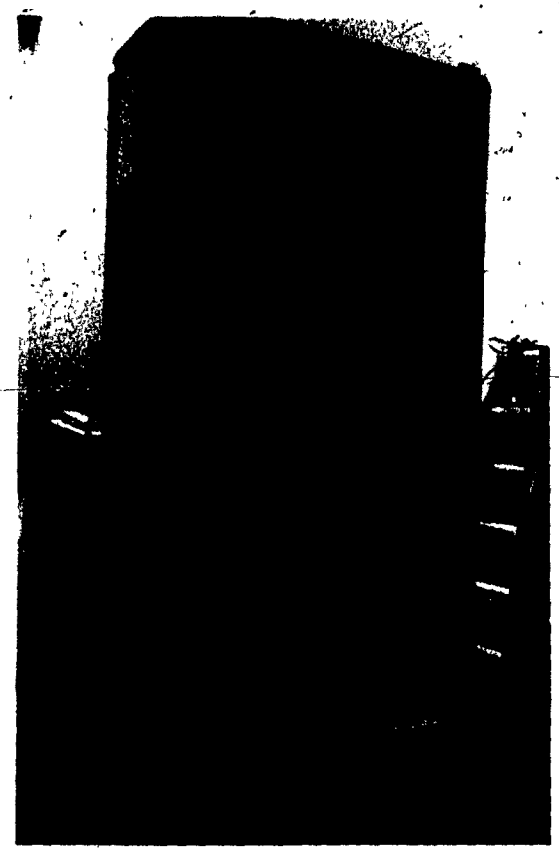

FIG. 3.13: COOLING SIDE OF THE HOT-BOX

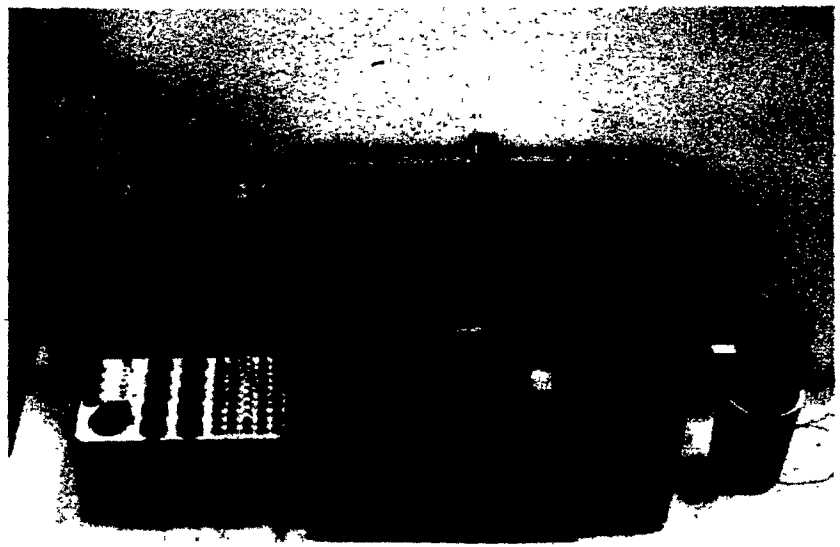

FIG. 3.14: POTENTIOMETER UNIT USED FOR TEMPERATURE MEASUREMENTS

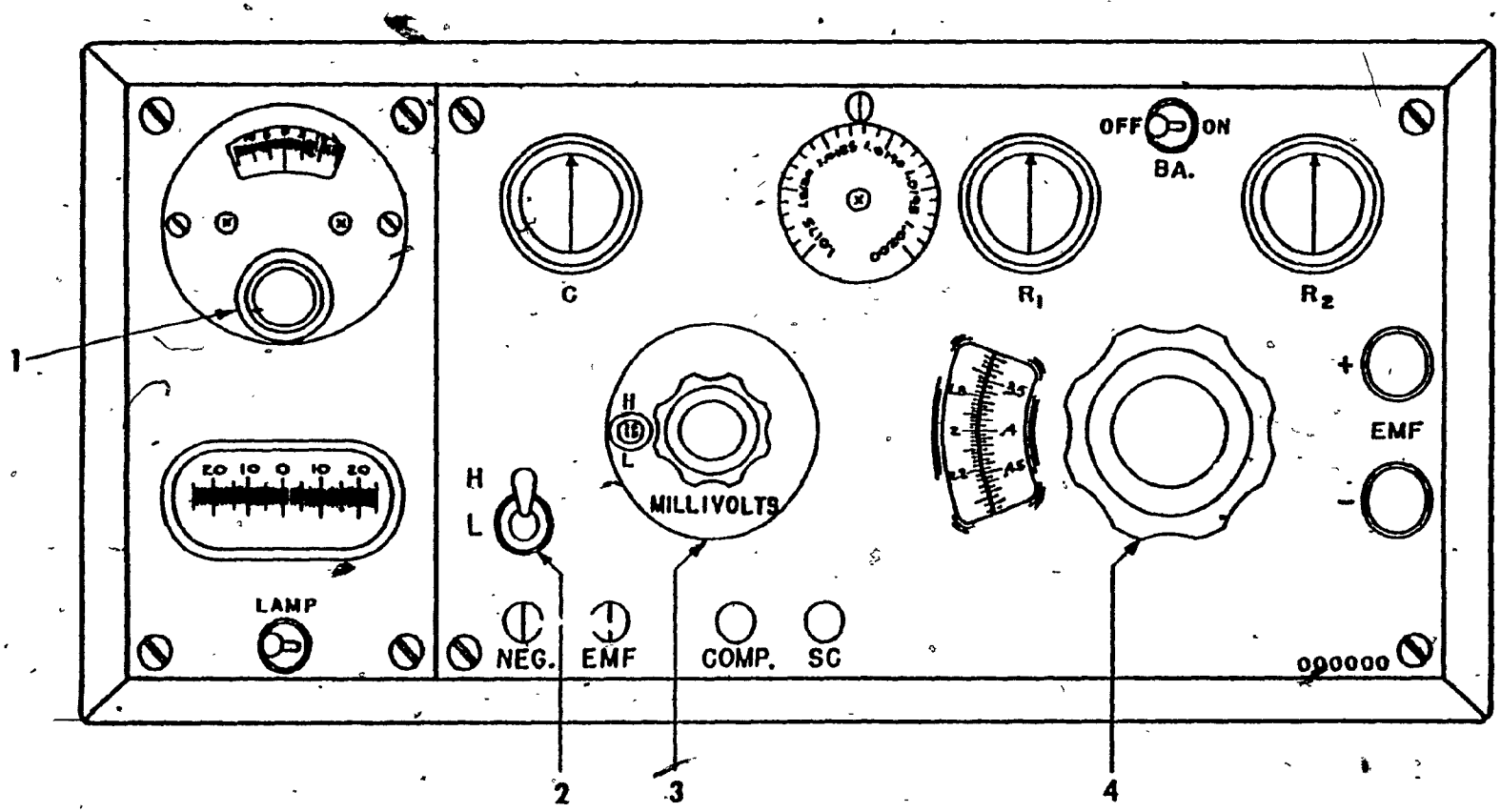

1. Adjustment Knob, Galvanometer
2. Range Switch
3. Step Switch
4. Slidewire

FIG. 3.15: TOP PANEL VIEW OF MODEL 2745

FIG. 3.16: THE SANDWICH SPECIMEN WHICH WAS USED FOR THERMAL STRESS MEASUREMENTS

FIG. 3.17: STRAIN GAGES POSITIONS ON THE SANDWICH SPECIMEN

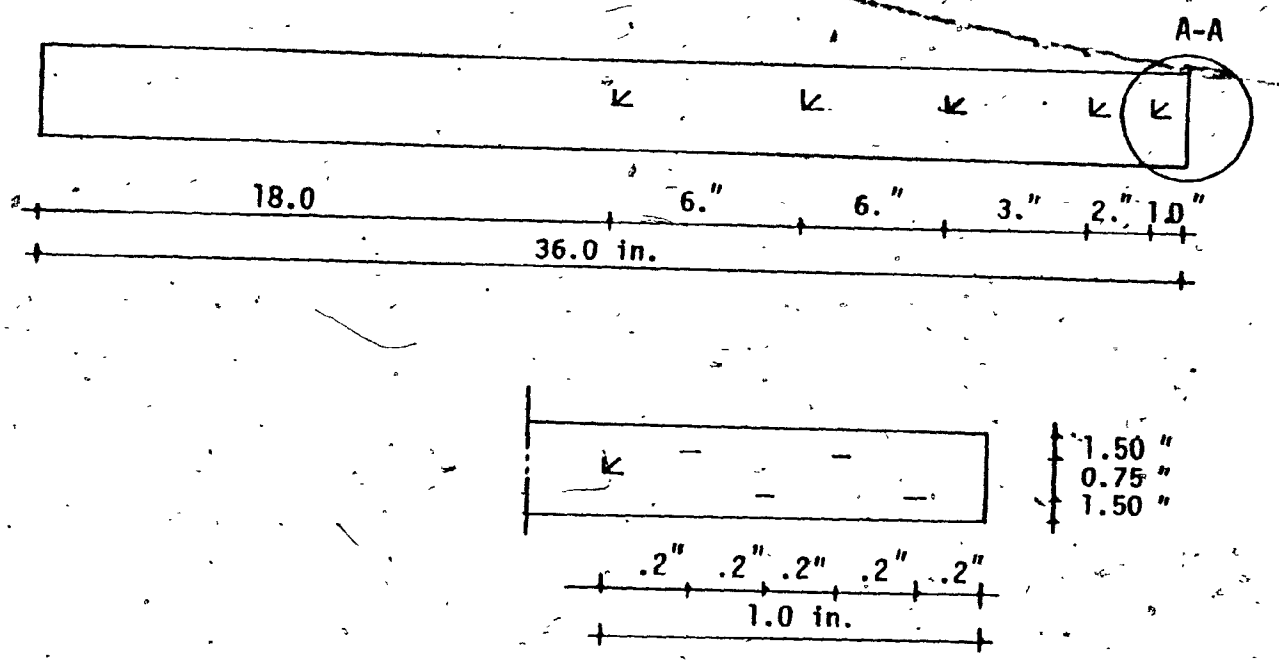

Details A-A (one face only)

FIG. 3.18: POSITIONS OF GAGES ALONG THE SANDWICH SAMPLE

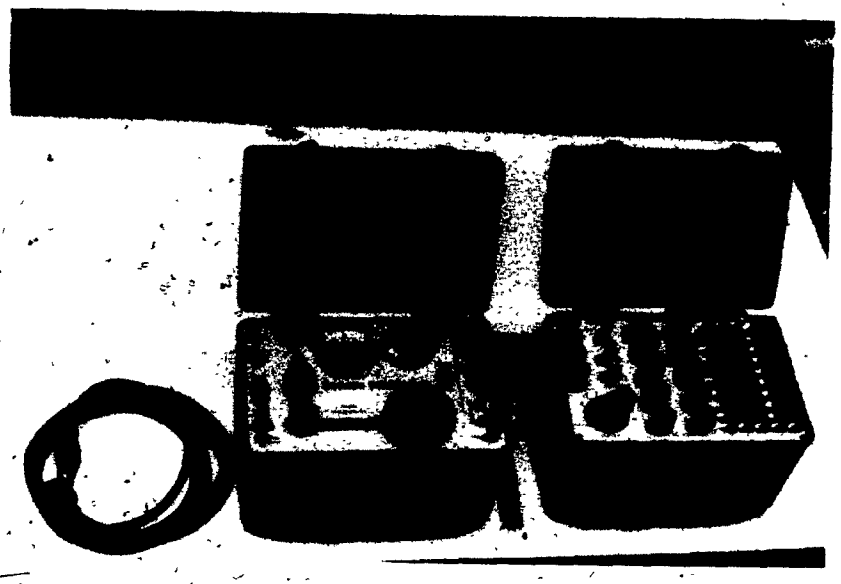

FIG. 3.19: STRAIN INDICATOR AND SWITCH UNITS WHICH WERE USED FOR THERMAL STRAIN MEASUREMENTS

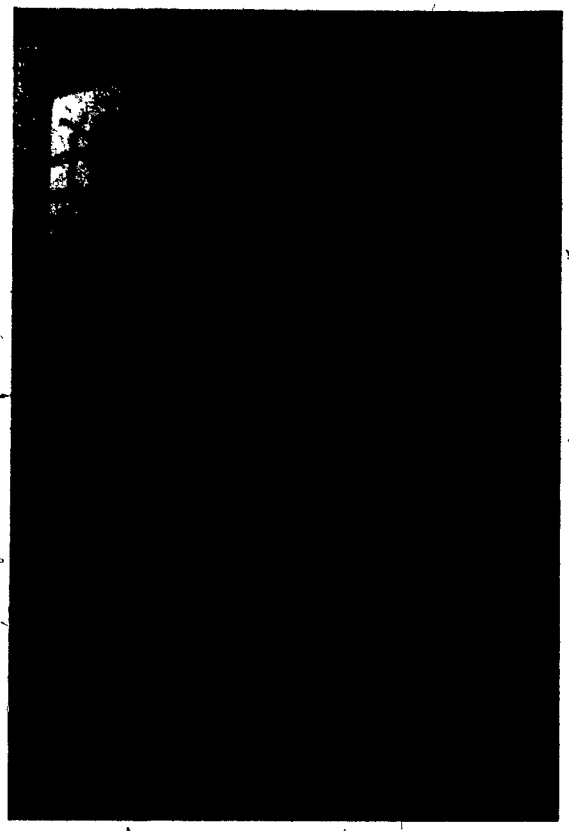

FIG. 3.20: A SANDWICH PLATE USED TO SUPPORT THE SANDWICH SPECIMEN

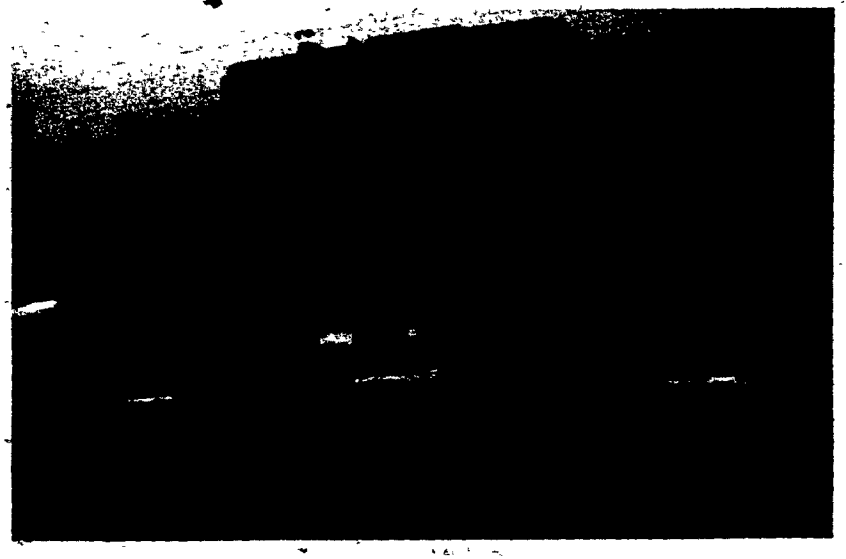

FIG. 3.21: THERMAL STRESS-EXPERIMENT SET-UP

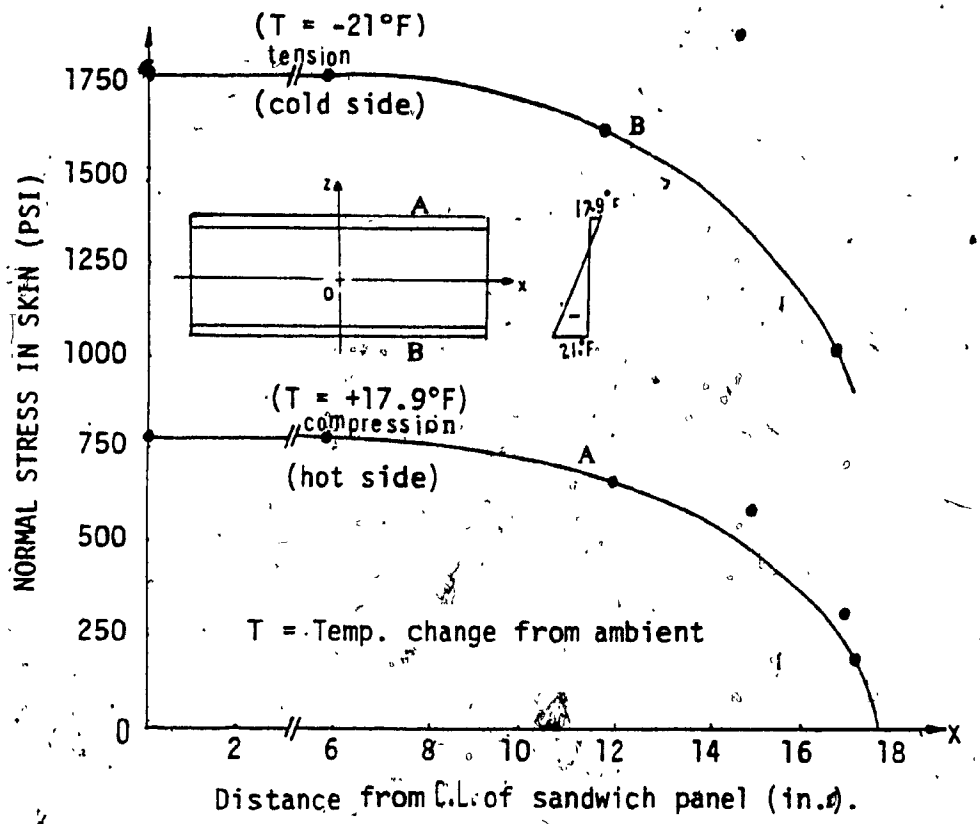

FIG. 3.22: SKIN, NORMAL STRESS
(Experimental results)

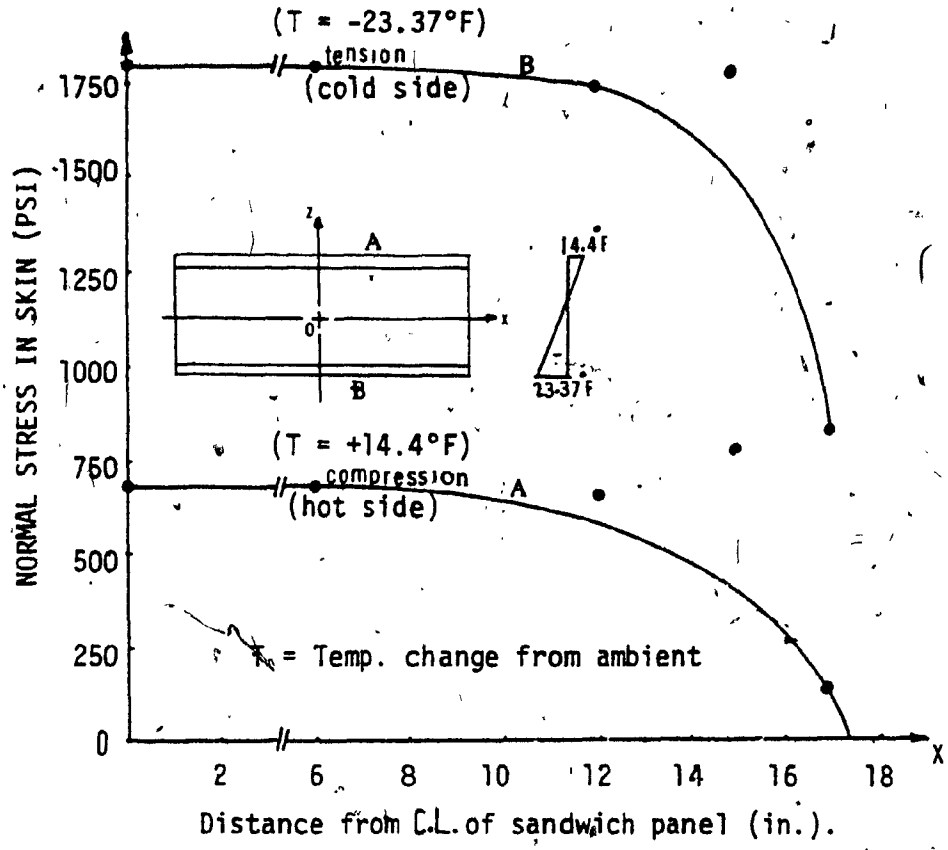

FIG. 3.23: SKIN, NORMAL STRESS
(Experimental results)

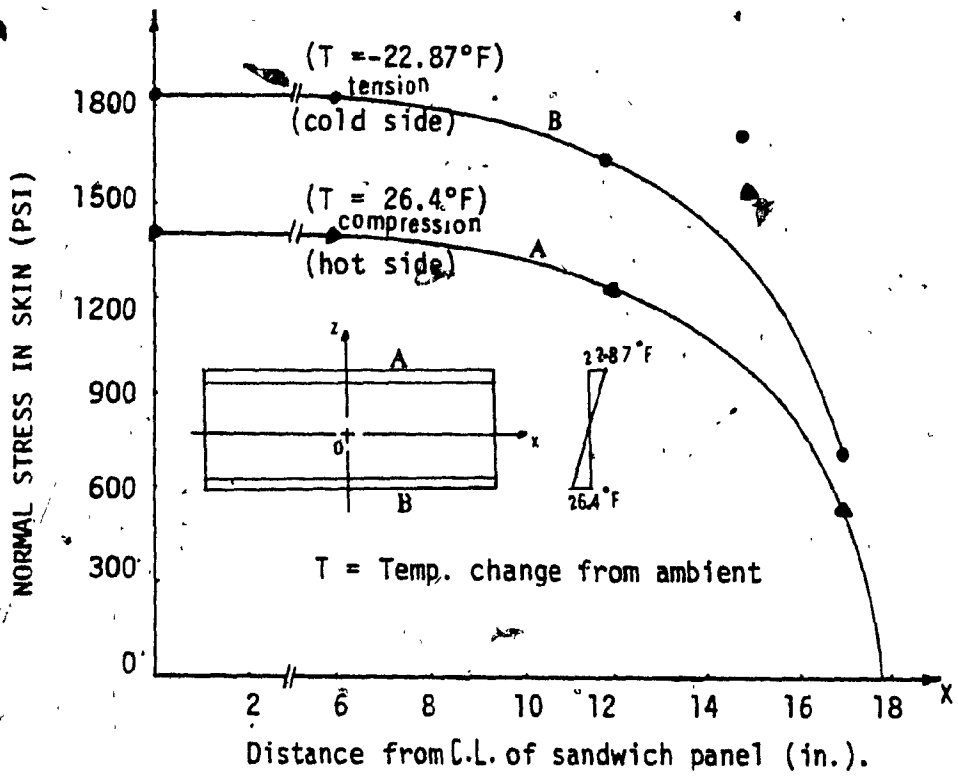

FIG. 3.24: SKIN, NORMAL STRESS
(Experimental results)

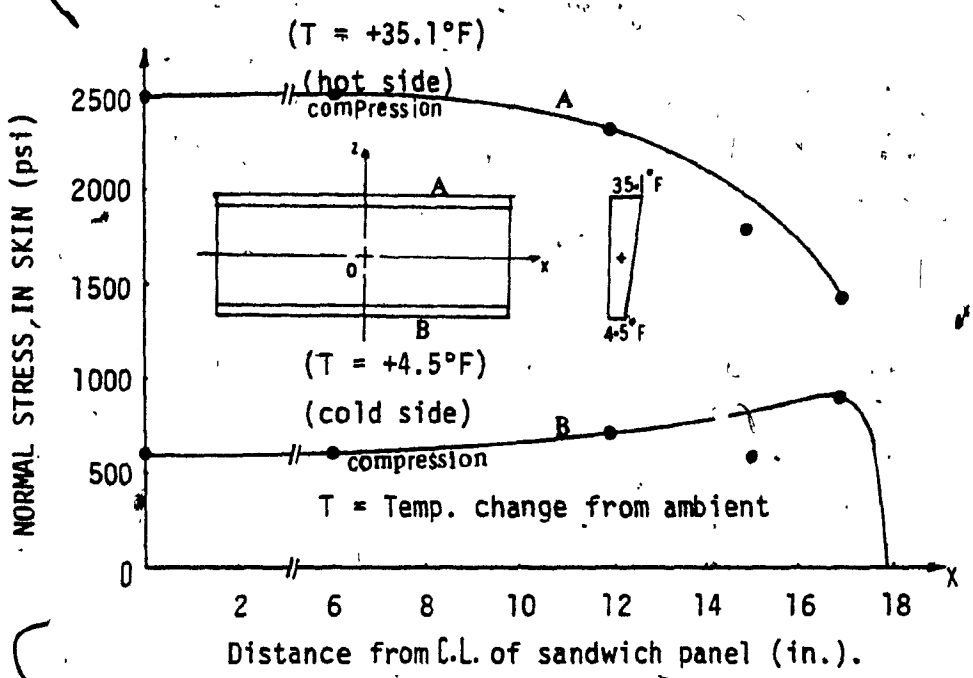

FIG. 3.25: SKIN, NORMAL STRESS
(Experimental results)

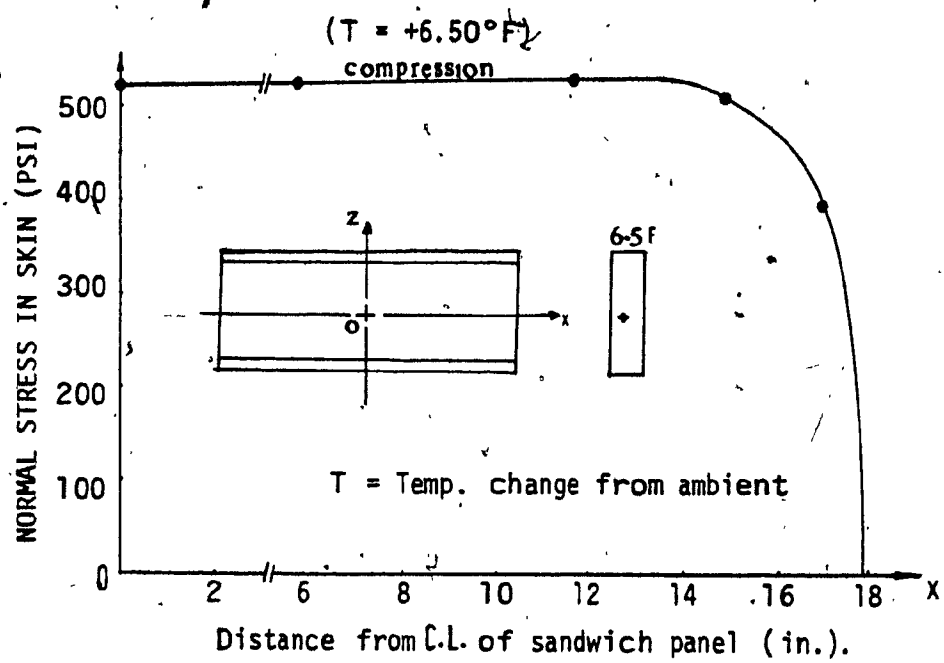

FIG. 3.26: SKIN, NORMAL STRESS

(Experimental results)

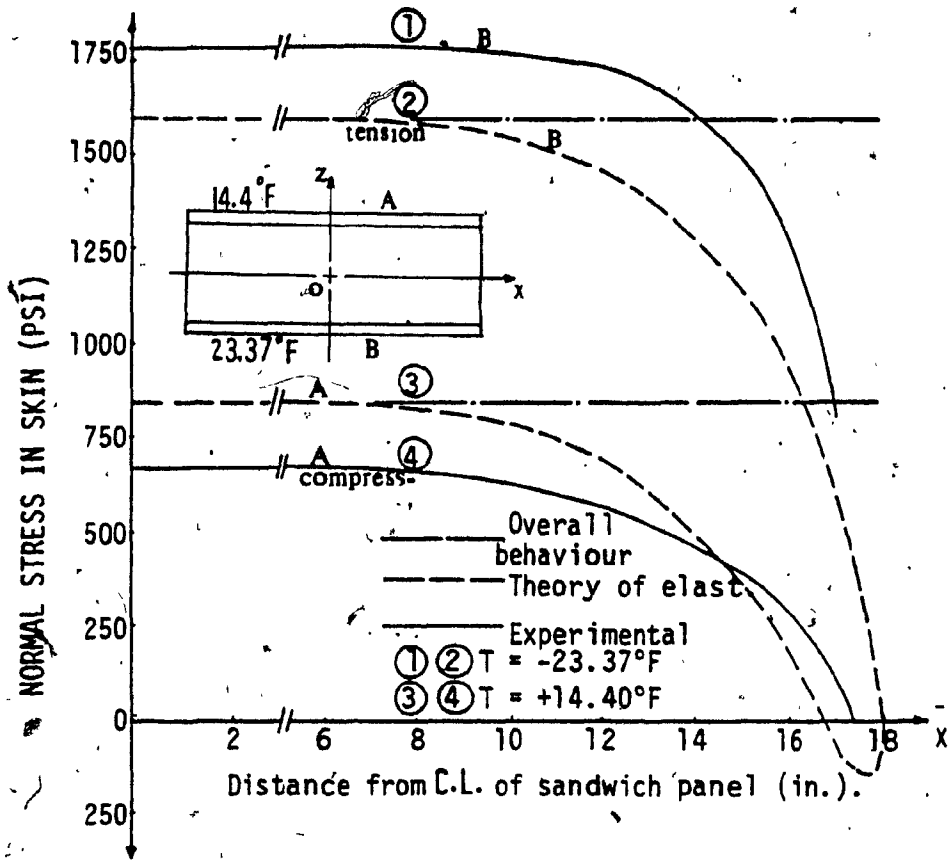

FIG. 4.1: SKIN, NORMAL STRESS

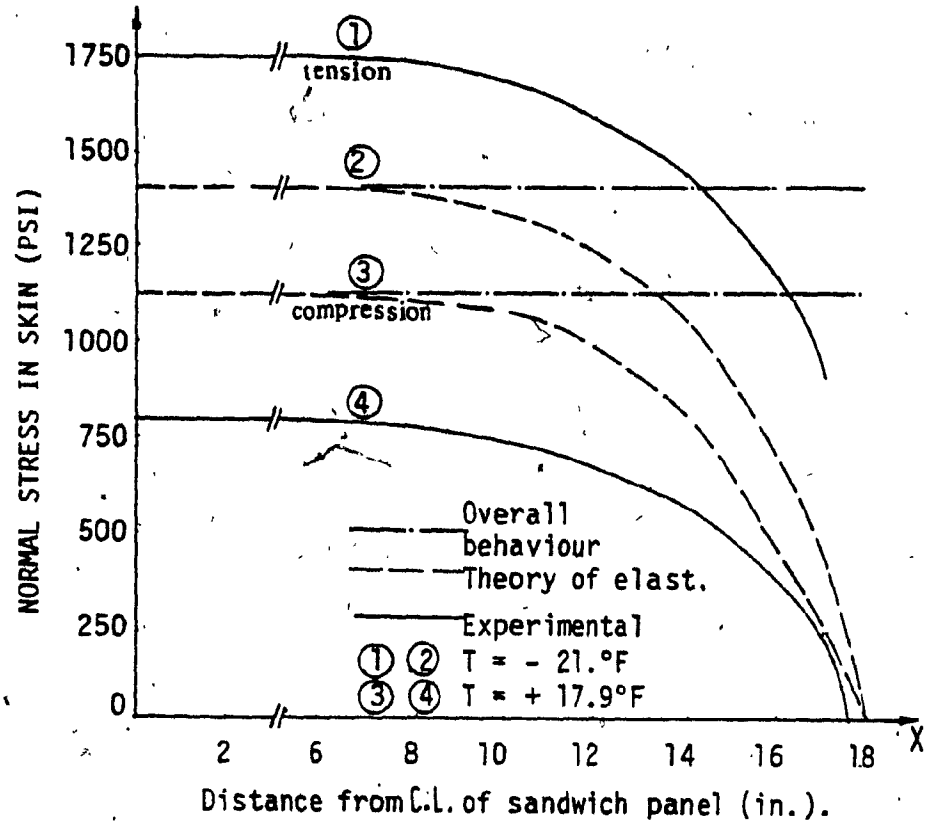

FIG. 4.2: SKIN, NORMAL STRESS

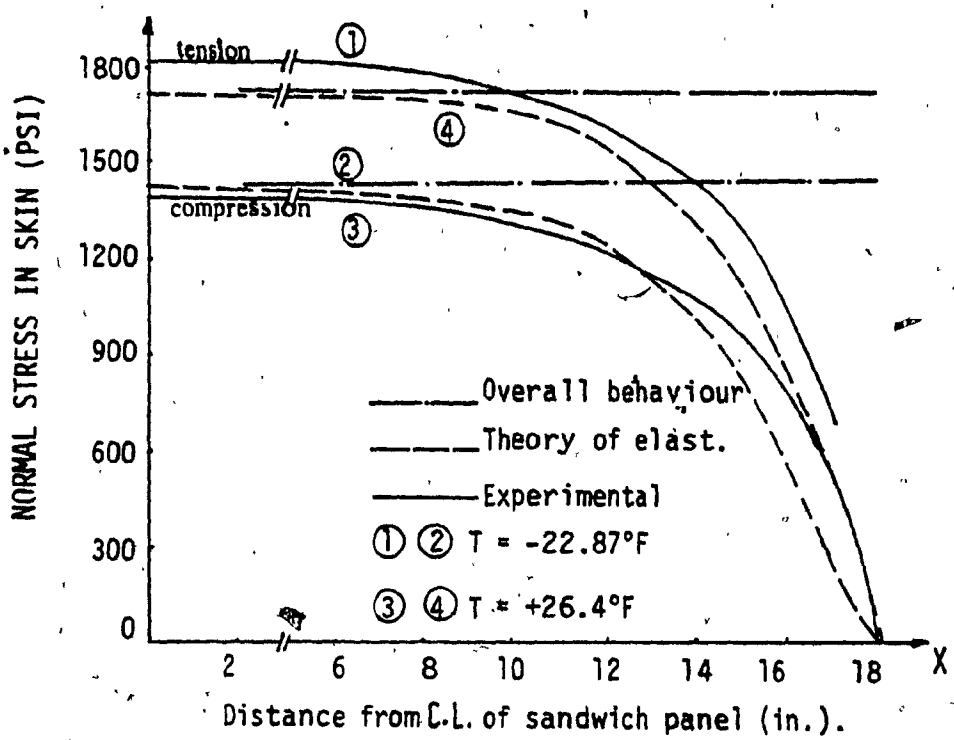

FIG. 4.3: SKIN, NORMAL STRESS

```
      READ 15,BY,D
      READ 15,G,77
15    FORMAT(2F15.6)
      C1=E2/G
      BMU=SQRT(C1)
      Y=0.
      DO 1555  I=1,73
      XX(I)=Y
1555  Y=Y+0.25
      ICODE=1
1373  READ 15,TEMPU,TEMPG
C
C**********
C**CALCULATING THE DISPLACEMENT AND THE STRESS DUE TO
C**UNIFORM TEMPERATURES.
C**********
C
      I=1
      X=0.00
40    GU=0.00
      DISPLU=0.00
      STRESU=0.00
      SHEEU=0.00
      SHEEG=0.00
      DO 20  N=1,105,2
      C2=(ALFA2-ALFA1)*(TEMPU*SPAN)
      NN=(N-1)/2
```

```
      C3=(-1.)**NN
      C4=8.*C3
      C5=C2*C4
      C6=(N**2)*(BY**2)
      C7=(2.*BMU*G*SPAN)/(N*BY*E1*THICK)
      C8=(BMU*N*BY*D)/(2.*SPAN)
      C9=(C7*SINH(C8))+(COSH(C8))
      ANU=C5/(C6*C9)
      C10=(N*BY*X)/(2.*SPAN)
      C11=(BMU*N*BY*D)/(2.*SPAN)
      C412=(ANU*SIN(C10)*SINH(C11))/N
      C567=(N)*(ANU)*(SIN(C10))*(SINH(C11))
      GU=GU+C567
      DISPLU=DISPLU+C412
      C12=ANU*COS(C10)*SINH(C11)
20    STRESU=STRESU+C12
      SHEEU=(BMU*G*BY*GU)/(2.*SPAN)
      C411=(2.*BMU*G*SPAN)/(BY*E1*THICK)
      DISPLU=C411*DISPLU
      STRESU=BMU*G*STRESU/THICK
C
C**********
C**CALCULATING THE DISPLACEMENT AND THE STRESS DUE TO
C**THE TEMPERATURE GRADIENT.
      GG=0.00
      DISPLG=0.00
      STRESG=0.00
      DO 50  N=1,105,2
      C20=1.+((D*E2)/(3.*THICK*E1))
      C21=(BMU*N*BY*D)/(2.*SPAN)
      C22=(C20)*(C21)
      C23=(N**2)*(BY**2)
```

```
      C24=(C23)*(SINH(C22))
      NNN=(N-1)/2
      C25=(8.)*((-1.)**NNN)
      C26=(ALFA2-ALFA1)*TEMPG*SPAN
      C27=(C25)*(C26)
      ANG=(C27)/(C24)
      C30=(N*BY*X)/(2.*SPAN)
      C40=(BMU*N*BY*D)/(2.*SPAN)
      C512=(ANG)*(SIN(C30))*(SINH(C40))
      C589=(N**2)*(ANG)*(SIN(C30))*(SINH(C40))
      GG=GG+C589
      DISPLG=DISPLG+C512
      C41=(N*ANG*(COS(C30))*(SINH(C40)))
50    STRESG=STRESG+C41
      C612=((D*E2)/(3.*THICK*E1))
      DISPLG=C612*DISPLG
      C689=((BY/(2.*SPAN))**2)*((D*E2)/3.)
      SHEEG=GG*C689
      STRESG=D*BY*E2*STRESG/(6.*THICK*SPAN)
      SHEU(I)=SHEEU
      SHEG(I)=SHEEG
      YH(I)=STRESU
      YC(I)=STRESG
      YYH(I)=DISPLU
      YYC(I)=DISPLG
```

```
      SHEH(I)=SHEU(I)+SHEG(I)
      SHEC(I)=SHEU(I)-SHEG(I)
      SH(I)=STRESU+STRESG
      SC(I)=STRESU-STRESG
      DISPH(I)=DISPLU+DISPLG
      DISPC(I)=DISPLU-DISPLG
      I=I+1
      X=XX(I)
      IF(I.LE.73) GO TO 40
C THE NORMAL STRESS FROM THE SLOPE OF THE DISPLACEMENT.
C THE SHEAR STRESS FROM THE SLOPE OF THE NORMAL STRESS.

      DO 1000  J=1,72
      STRESSU(J)=E1*(YYH(J)-YYH(J+1))/(XX(J)-XX(J+1))
      STRESSG(J)=E1*(YYC(J)-YYC(J+1))/(XX(J)-XX(J+1))
      STRESSH(J)=STRESSU(J)+STRESSG(J)
      STRESSC(J)=STRESSU(J)+STRESSG(J)
      ZZ=(XX(J)+XX(J+1))/2.
      XXX(J)=ZZ
1000  CONTINUE
17    PRINT 1321
1321  FORMAT(1H1,///,13X,*TABLE 2.1*,/,4X,*UNIFORM AND GRADIENT NORMAL
     1STRESSES*,/,4X,*AS EVALUATED FROM EQUATIONS 2.15 AND 2.21*)
      PRINT 5999
5999  FORMAT(1X,42(1H*))
      PRINT 6000
6000  FORMAT(2X,*UNIFORM STRESS*,2X,*GRAD STRESS*,4X,*POSITIONS*)
      PRINT 5999
      DO 6100  I=1,73
      IF(I/25*25 .EQ. I) PRINT 3415
      PRINT 2120,YH(I),YC(I),XX(I)
6100  CONTINUE
```

```
      PRINT 5999
      PRINT 1219
1219  FORMAT(1H1,///,13X,*TABLE 2.4*,/,7X,*SKIN NORMAL STRESSES*)
      PRINT 5999
      PRINT 1220
1220  FORMAT(2X,*COLD STRESS*,5X,*HOT STRESS*,5X,*POSITIONS*)
      PRINT 5999
      DO 1320  I=1,73
      IF(I/25*25 .EQ. I) PRINT 3415
      PRINT 1120,SC(I),SH(I),XX(I)
1320  CONTINUE
      PRINT 5999
1120  FORMAT(1X,1H*,F10.5,2X,1H*,2X,F10.3,2X,1H*,2X,F10.5,1H*)
      PRINT 5001
      PRINT 5999
      PRINT 5002
      PRINT 5999
5001  FORMAT(1H1,///,13X,*TABLE 2.2*,/,4X,*UNIFORM AND GRAD SHEAR
     1STRESSES*,/,4X,*AS EVALUATED FROM EQUS. 2.14 AND 2.22*)
5002  FORMAT(2X,*UNIFORM SHEAR*,2X,*GRAD SHEAR*,4X,*POSITIONS*)
      DO 100  I=1,73
      IF(I/25*25 .EQ. I) PRINT 3415
      PRINT 2120,SHEU(I),SHEG(I),XX(I)
100   CONTINUE
      PRINT 5999
```

```
2120  FORMAT(1X,1H*,F10.5,2X,1H*,2X,F10.3,2X,1H*,2X,F10.5,1H*)
      PRINT 6199
6199  FORMAT(1H1,///,13X,*TABLE 2.5*,/,7X,*SHEAR STRESS IN THE GLUE
     1LINE*)
      PRINT 5999
      PRINT 6200
6200  FORMAT(2X,*COLD SHEAR*,5X,*HOT SHEAR*,5X,*POSITIONS*)
      PRINT 5999
      DO 7100  I=1,73
      IF(I/25*25 .EQ. I) PRINT 3415
      PRINT 2120,SHEC(I),SHEH(I),XX(I)
7100  CONTINUE
      PRINT 5999
      PRINT 5004
5004  FORMAT(1H1,///,13X,*TABLE 2.3*,/,4X,*UNIFORM AND GRADIENT SKIN
     1DISPACEMENTS AS*,/,4X,*EVALUATED FROM EQUS. 2.13 AND 2.18*)
      PRINT 5999
      PRINT 5003
5003  FORMAT(2X,*UNIFORM DISPL*,2X,*GRAD DISPL*,4X,*POSITIONS*)
      PRINT 5999
      DO 300  I=1,73
      IF(I/25*25 .EQ. I) PRINT 3415
      PRINT 2120,YYH(I),YYC(I),XX(I)
300   CONTINUE
      PRINT 5999
      PRINT 8999
8999  FORMAT(1H1,///,13X,*TABLE 2.6*,/,7X,*SKIN DISPLACEMENTS*)
      PRINT 5999
      PRINT 9000
9000  FORMAT(2X,*COLD DISPL.*,2X,*HOT DISPL.*,4X,*POSITIONS*)
```

```
      PRINT 5999
      DO 9100  I=1,73
      IF(I/25*25 .EQ. I) PRINT 3415
      PRINT 2120, DISPC(I),DISPH(I),XX(I)
9100  CONTINUE
      PRINT 5999

      DO 1001  J=1,71
      SHEARU(J)=(STRESSU(J)-STRESSU(J+1))/(XXX(J+1)-XXX(J))
      SHEARG(J)=(STRESSG(J)-STRESSG(J+1))/(XXX(J+1)-XXX(J))
      SHEARU(J)=SHEARU(J)*0.025
      SHEARG(J)=SHEARG(J)*0.025
      SHEARH(J)=SHEARU(J)+SHEARG(J)
      SHEARC(J)=SHEARU(J)-SHEARG(J)
1001  CONTINUE
      PRINT 1322
1322  FORMAT(1H1,///,13X,*TABLE 2.7*,/,7X,*SKIN NORMAL STRESSES*,/,7X,
     1*USING EQUATION 2.11*)
      PRINT 5999
      PRINT 1004
1004  FORMAT(2X,*UNIFORM STRESS*,2X,*GRAD STRESS*,4X,*POSITIONS*)
      PRINT 5999
      DO 1111  J=1,72
      IF(J/25*25 .EQ. J) PRINT 3415
      PRINT 1120,STRESSU(J),STRESSG(J),XXX(J)
1111  CONTINUE
      PRINT 5999
```

```
      PRINT 1002
1002  FORMAT(1H1,///,13X,*TABLE 2.8*,/,7X,*SKIN NORMAL STRESSES*,/,7X,
     1*USING EQUATION 2.24*)
      PRINT 5999
      PRINT 1005
1005  FORMAT(2X,*COLD STRESS*,2X,*HOT STRESS*,4X,*POSITIONS*)
      PRINT 5999
      DO 1006  J=1,72
      IF(J/25*25 .EQ. J) PRINT 3415
      PRINT 1120,STRESSH(J),STRESSC(J),XXX(J)
1006  CONTINUE
      PRINT 5999
      PRINT 1589
1589  FORMAT(1H1,///,13X,*TABLE 2.9*,/,7X,*SHEAR STRESS IN GLUE*,/,
     17X,*LINE USING EQUATION 2.120*)
      PRINT 5999
      PRINT 1007
1007  FORMAT(2X,*UNIFORM SHEAR*,2X,*GRAD SHEAR*,4X,*POSITIONS*)
      PRINT 5999
      DO 1008  J=1,71
      IF(J/25*25 .EQ. J) PRINT 3415
      PRINT 1120,SHEARU(J),SHEARG(J),XX(J+1)
1008  CONTINUE
```

```
      PRINT 5999
      PRINT 1319
1319  FORMAT(1H1,///,13X,*TABLE 2.10*,/,4X,*SHEAR STRESS IN GLUE LINE*)
      PRINT 5999
      PRINT 1009
1009  FORMAT(2X,*COLD SHEAR*,2X,*HOT SHEAR*,4X,*POSITIONS*)
      PRINT 5999
      DO 1010   J=1,71
      IF(J/25*25 .EQ. J) PRINT 3415
      PRINT 1120, SHEARC(J),SHEARH(J),XX(J+1)
1010  CONTINUE
      PRINT 5999
      PRINT 5962
5962  FORMAT(1X,120(1H*))
23    ICODE=ICODE+1
      IF(ICODE .LE. 5) GO TO 1373
3415  FORMAT(1X,42(1H*),///,13X,*TABLE 2.   (CONTINUE)*,/,
     142(1H*))
      STOP
      END
```

APPENDIX B

DERIVATION OF ELEMENT STIFFNESS MATRIX [K]

$$k_{11} = tab\int_0^1\int_0^1 \frac{E_{xx}(1-\eta)^2}{a^2\lambda} + \frac{G_{xz}(1-\xi)^2}{b^2}\, d\xi d\eta = tab\left(\frac{E_{xx}}{3a^2\lambda} + \frac{G_{xz}}{3b^2}\right)$$

$$k_{12} = tab\int_0^1\int_0^1 \frac{\nu_{xx}E_{xx}(1-\xi)(1+\eta)}{ab\lambda} + \frac{G_{xz}(1-\xi)(1-\eta)}{ab}\, d\xi d\eta$$

$$= tab\left(\frac{\nu_{zx}E_{xx}}{4ab\lambda} + \frac{G_{xz}}{4ab}\right)$$

$$k_{13} = tab\int_0^1\int_0^1 \frac{-E_{xx}(1-\eta)^2}{a^2\lambda} + \frac{G_{xz}(1-\xi)\xi}{ab}\, d\xi d\eta = tab\left(\frac{-E_{xx}}{3a^2\lambda} + \frac{G_{xz}}{6b^2}\right)$$

$$k_{14} = tab\int_0^1\int_0^1 \frac{\nu_{zx}E_{xx}\xi(1-\eta)}{ab\lambda} - \frac{G_{xz}(1-\xi)(1-\eta)}{ab}\, d\xi d\eta = tab\left(\frac{\nu_{zx}E_{xx}}{4ab\lambda} - \frac{G_{xz}}{4ab}\right)$$

$$k_{15} = tab\int_0^1\int_0^1 \frac{-E_{xx}\eta(1-\eta)}{a^2\lambda} - \frac{G_{xz}(1-\xi)\xi}{b^2}\, d\xi d\eta = tab\left(\frac{-E_{xx}}{6a^2\lambda} - \frac{G_{xz}}{6b^2}\right)$$

$$k_{16} = tab\int_0^1\int_0^1 \frac{-\nu_{zx}E_{xx}(1-\eta)\xi}{ab\lambda} - \frac{G_{xz}(1-\xi)\eta}{ab}\, d\xi d\eta$$

$$= tab\left(\frac{-\nu_{zx}E_{xx}}{4ab\lambda} - \frac{G_{xz}}{4ab}\right)$$

$$k_{17} = tab\int_0^1\int_0^1 \frac{E_{xx}(1-\eta)\eta}{a^2\lambda} - \frac{G_{xz}(1-\xi)^2}{b^2}\, d\xi d\eta = tab\left(\frac{E_{xx}}{6a^2\lambda} - \frac{G_{xz}}{3b^2}\right)$$

$$k_{18} = tab\int_0^1\int_0^1 \frac{-\nu_{zx}E_{xx}(1-\xi)(1-\eta)}{ab\lambda} + \frac{G_{xz}(1-\xi)\eta}{ab}\, d\xi d\eta$$

$$= tab\left(\frac{-\nu_{zx}E_{xx}}{4ab\lambda} + \frac{G_{xz}}{4ab}\right)$$

$$k_{22} = tab\int_0^1\int_0^1 \frac{E_{zz}(1-\xi)^2}{b^2\lambda} + \frac{G_{xz}(1-\eta)^2}{\alpha^2}\, d\xi d\eta = tab\left(\frac{E_{zz}}{3b^2\lambda} + \frac{G_{xz}}{3a^2}\right)$$

$$k_{23} = tab\int_0^1\int_0^1 \frac{-\nu_{xz}E_{zz}(1-\xi)(1-\eta)}{ab\lambda} + \frac{G_{xz}(1-\eta)\xi}{ab}\, d\xi d\eta =$$

$$= tab\left(\frac{-\nu_{xz}E_{zz}}{4ab\lambda} + \frac{G_{xz}}{4ab}\right)$$

$$k_{24} = tab\int_0^1\int_0^1 \frac{E_{zz}(1-\xi)\xi}{b^2\lambda} - \frac{G_{xz}(1-\eta)^2}{a^2}\, d\xi d\eta = tab\left(\frac{E_{zz}}{6b^2\lambda} - \frac{G_{xz}}{3a^2}\right)$$

$$k_{25} = tab\int_0^1\int_0^1 \frac{-\nu_{xz}E_{zz}(1-\xi)\eta}{ab\lambda} - \frac{G_{xz}(1-\eta)\xi}{ab}\, d\xi d\eta = tab\left(\frac{-\nu_{xz}E_{zz}}{4ab\lambda} - \frac{G_{xz}}{4ab}\right)$$

$$k_{26} = tab\int_0^1\int_0^1 \frac{-E_{zz}(1-\xi)\xi}{b^2\lambda} - \frac{G_{xz}(1-\eta)\eta}{a^2}\, d\xi d\eta = tab\left(\frac{-E_{zz}}{6b^2\lambda} - \frac{G_{xz}}{6a^2}\right)$$

$$k_{27} = tab\int_0^1\int_0^1 \frac{\nu_{xz}E_{zz}(1-\xi)\eta}{4ab\lambda} - \frac{G_{xz}(1-\eta)(1-\xi)}{ab}\, d\xi d\eta$$

$$= tab\left(\frac{\nu_{xz}E_{zz}}{4ab\lambda} - \frac{G_{xz}}{4ab}\right)$$

$$k_{28} = tab\int_0^1\int_0^1 -E_{zz}(1-\xi)^2 + G_{xz}(1-\eta)\eta\, d\xi d\eta = tab\left(\frac{-E_{zz}}{3b^2\lambda} + \frac{G_{xz}}{6a^2}\right)$$

$$k_{33} = tab\int_0^1\int_0^1 \frac{E_{xx}(1-\eta)^2}{a^2\lambda} + G_{xz}\frac{\xi^2}{b^2}\, d\xi d\eta = tab\left(\frac{E_{xx}}{3a^2\lambda} + \frac{G_{xz}}{3b^2}\right)$$

$$k_{34} = tab\int_0^1\int_0^1 \frac{-\nu_{zx}E_{xx}(1-\eta)\xi}{ab\lambda} - \frac{G_{xz}(1-\eta)\xi}{ab}\, d\xi d\eta = tab\left(\frac{-\nu_{zx}E_{xx}}{4ab\lambda} - \frac{G_{xz}}{4ab}\right)$$

$$k_{35} = tab\int_0^1\int_0^1 \frac{E_{xx}(1-\eta)\eta}{a^2\lambda} - G_{xz}\frac{\xi^2}{b^2}\, d\xi d\eta = tab\left(\frac{E_{xx}}{6a^2\lambda} - \frac{G_{xz}}{3b^2}\right)$$

$$k_{36} = tab\int_0^1\int_0^1 \frac{\nu_{zx}E_{xx}(1-\eta)\xi}{ab\lambda} - \frac{G_{xz}\xi\eta}{ab}\, d\xi d\eta = tab\left(\frac{\nu_{zx}E_{xx}}{4ab\lambda} - \frac{G_{xz}}{4ab}\right)$$

$$k_{37} = tab\int_0^1\int_0^1 \frac{-E_{xx}(1-\eta)\eta}{a^2\lambda} - \frac{G_{xz}(1-\xi)\xi}{b^2}\, d\xi d\eta = tab\left(\frac{-E_{xx}}{6a^2\lambda} - \frac{G_{xz}}{6b^2}\right)$$

$$k_{38} = tab\int_0^1\int_0^1 \frac{\nu_{zx}E_{xx}(1-\eta)(1-\xi)}{ab\lambda} + \frac{G_{xz}\xi\eta}{ab}\, d\xi d\eta = tab\left(\frac{\nu_{zx}E_{xx}}{4ab\lambda} + \frac{G_{xz}}{4ab}\right)$$

$$k_{44} = tab\int_0^1\int_0^1 \frac{E_{zz}\xi^2}{\lambda b^2} + \frac{G_{xz}(1-\eta)^2}{a^2}\, d\xi d\eta = tab\left(\frac{E_{zz}}{3b^2\lambda} + \frac{G_{xz}}{3a^2}\right)$$

$$k_{45} = tab\int_0^1\int_0^1 \frac{-\nu_{xz}E_{zz}\xi\eta}{ab\lambda} + \frac{G_{xz}(1-\eta)\xi}{ab}\, d\xi d\eta = tab\left(\frac{-\nu_{xz}E_{zz}}{4ab\lambda} + \frac{G_{xz}}{4ab}\right)$$

$$k_{40} = tab\int_0^1\int_0^1 \frac{-E_{zz}\xi^2}{\lambda b^2} + \frac{G_{xz}(1-\eta)\eta}{a^2}\, d\xi d\eta = tab\left(\frac{-E_{zz}}{3b^2\lambda} + \frac{G_{xz}}{6a^2}\right)$$

$$k_{47} = tab\int_0^1\int_0^1 \frac{(\nu_{xz}E_{zz}\xi\eta)}{ab\lambda} + \frac{G_{xz}(1-\xi)(1-\eta)}{ab}\, d\xi d\eta = tab\left(\frac{\nu_{xz}E_{zz}}{4ab\lambda} + \frac{G_{xz}}{4ab}\right)$$

$$k_{48} = tab\int_0^1\int_0^1 \frac{-E_{zz}(1-\xi)\xi}{b^2\lambda} - \frac{G_{xz}(1-\eta)\eta}{a^2}\, d\xi d\eta = tab\left(\frac{-E_{zz}}{4ab\lambda} - \frac{G_{xz}}{4ab}\right)$$

$$k_{55} = tab\int_0^1\int_0^1 \frac{E_{xx}\eta^2}{a^2\lambda} + \frac{G_{xz}\xi^2}{b^2}\, d\xi d\eta = tab\left(\frac{E_{xx}}{3a^2\lambda} + \frac{G_{xz}}{3b^2}\right)$$

$$k_{56} = tab\int_0^1\int_0^1 \frac{\nu_{zx}E_{xx}\xi\eta}{ab\lambda} + \frac{G_{xz}\xi\eta}{ab}\, d\xi d\eta = tab\left(\frac{\nu_{zx}E_{xx}}{4ab\lambda} + \frac{G_{xz}}{4ab}\right)$$

$$k_{57} = tab\int_0^1\int_0^1 \frac{-E_{xx}\eta^2}{a^2\lambda} + \frac{G_{xz}(1-\xi)\xi}{b^2}\, d\xi d\eta = tab\left(\frac{-E_{xx}}{3a^2\lambda} + \frac{G_{xz}}{6b^2}\right)$$

$$k_{58} = tab\int_0^1\int_0^1 \frac{\nu_{xz}E_{xx}(1-\xi)\eta}{ab\lambda} - \frac{G_{xz}\xi\eta}{ab}\, d\xi d\eta = tab\left(\frac{\nu_{zx}E_{xx}}{4ab\lambda} - \frac{G_{xz}}{4ab}\right)$$

$$k_{66} = tab\int_0^1\int_0^1 \frac{E_{zz}\xi^2}{\lambda b^2} + \frac{G_{xz}\eta^2}{a^2}\, d\xi d\eta = tab\left(\frac{E_{zz}}{3\lambda b^2} + \frac{G_{xz}}{3a^2}\right)$$

$$k_{67} = tab\int_0^1\int_0^1 \frac{-\nu_{xz}E_{zz}\xi\eta}{ab\lambda} + \frac{G_{xz}(1-\xi)\eta}{ab}\, d\xi d\eta = tab\left(\frac{-\nu_{xz}E_{zz}}{4ab\lambda} + \frac{G_{xz}}{4ab}\right)$$

$$k_{68} = tab\int_0^1\int_0^1 \frac{E_{zz}(1-\xi)\xi}{b^2\lambda} - \frac{G_{xz}\eta^2}{a^2}\, d\xi d\eta = tab\left(\frac{E_{zz}}{6b^2\lambda} - \frac{G_{xz}}{3a^2}\right)$$

$$k_{77} = tab\int_0^1\int_0^1 \frac{E_{xx}\eta^2}{a^2\lambda} + \frac{G_{xz}(1-\xi)^2}{b^2}\, d\xi d\eta = tab\left(\frac{E_{xx}}{3a^2\lambda} + \frac{G_{xz}}{3b^2}\right)$$

$$k_{78} = tab\int_0^1\int_0^1 \frac{-\nu_{zx}E_{xx}(1-\xi)\eta}{ab\lambda} - \frac{G_{xz}(1-\xi)\eta}{ab}\, d\xi d\eta = tab\left(\frac{-\nu_{zx}E_{xx}}{4ab\lambda} - \frac{G_{xz}}{4ab}\right)$$

$$k_{88} = tab\int_0^1\int_0^1 \frac{E_{zz}(1-\xi)^2}{b^2\lambda} + \frac{G_{xz}\eta^2}{a^2}\, d\xi d\eta = tab\left(\frac{E_{zz}}{3b^2\lambda} + \frac{G_{xz}}{3a^2}\right)$$

APPENDIX C

MATERIAL PROPERTIES

MATERIAL PROPERTIES

F.1 ALUMINIUM

The aluminium which was used as skins for the sandwich specimen is alloy 3003, produced by Alcan Canada Limited [6]. It has the following properties:

Thickness	=	0.025 in.
Modulus of elasticity	=	$10.^4$ ksi
Shear modulus of elasticity	=	$0.4 \times 10.^4$ ksi
Poisson's ratio	=	0.33
Coefficient of linear expansion	=	13×10^{-6} /°F

F.2 WHITE PINE WOOD

F.2.1 SHEAR MODULUS

No standard exists to calculate the shear modulus of the wood, therefore, this experiment was done depending on the elementary mechanics of materials.

The angle of twist for a straight bar, uniform, circular section and loaded by equal and opposite twisting couples, can determine from the relation:

$$\theta = \frac{TL}{JG}$$

where T = twisting moment

L = length of the member

J = polar moment of inertia of the cross section

G = modulus of rigidity of the bar material

θ = angle of twist (radians)

Three specimens are prepared from the same wood which was used as a sandwich core in this research, each sample has the same shape, Figs. (C.1) and (C.2) and the actual dimensions were as follows:

Sample	d1(mm) average three measurements	d2 (mm)	L (mm)	a1, a2 (mm)
A	9.08	125	121	37.50, 37.25
B	9.01	126	120.6	37.90, 38.60
C	9.307	134	120.72	38.30, 38.20

By using the testing machine, INSTRON, (FIG. (C.3)), which is available at the university, the following were test procedures to determine shear rigidity for pine wood.

- the torsion load cell installed, wood specimen inserted into it and the chuck hand tightened, Fig. (C.4).
- the drawing pen set to zero reference line (the full left reference zero selected to represent the zero reference.).
- the load weighing system balanced and calibrated against precise load signal. The system calibration for all ranges of the load cell set in use.
- the crosshead and the chart speeds chosen.
- the power knob switched ON.

The average shear rigidity is 130.819 kg/mm^2 or 186086.771 psi and this was the shear rigidity value used in the mathematical analysis. Chapter II, or, in the finite element analysis, (Figs.(C.5) and(C.6) show the graphs of this test).

C2.2 MODULUS OF ELASTICITY

A straight wood beam of rectangular cross section is subjected to a bending moment by supporting it near its ends and applying transverse two loads symmetrically imposed between these two supports (Fig. (C.7)). The coordinate observations of loads and deflections are made until rupture occured (one of the objectives of two point loading is to subject the portion of the beam between load points to a uniform bending moment, free of shear, and with comparatively small loads at the load points. For example, loads applied at one-third span length from reactions would be less than if applied at one-fourth span length from reaction to develop a moment of a similar magnitude). The following were the actual specimen dimensions as measured (Figs. C.8 and C.9):

Beam depth	=	b	= 3.721 (in.)
Beam width	=	a	= 1.739 (in.)
Beam span	=	L	= 27.0 (in.)
Total length	=	TL	= 33.0 (in.)

By using TINIUS OLSEN testing machine (Fig. (C.10)), the following were test procedures to determine modulus of elasticity of white pine wood:

- the flexure specimen supported at its reaction points on the testing machine plateform, as shown in Fig. (C.11). The supports were such that shortening and rotation of the specimen due to deflection will be unrestricted Figs. (C.12) and (C.13)
- full contact between support bearings, loading blocks and the specimen surfaces attained.
- two dial gages are used: one to measure deflection at the center of the span and the other at one of the reaction points. Each dial gage permits measurements to the nearest 0.001 in.
- The specimen loaded continuously while the load values and the dial gages readings were recording. The specimen failed by cracking at its upper fibres at the center of its span, Fig. (C.14) (no crushing occurred), and the test stopped when the obtained load-deflection curve exceeded its straight line portion.
- the load deflection curve is shown in Fig. (C.15), from which

$$E = \left(\frac{Pa}{\Delta_{max}}\right)\left(\frac{3L^2-4a^2}{24I}\right)$$

$$= K.\frac{P}{\Delta_{max}}$$

$$= 428\,\frac{P}{\Delta_{max}}$$

$$= 1590000.\ \text{psi}$$

where K = constant

L = specimen span = 27 in.

$a = \frac{L}{3} = \frac{1}{2}$ shear span

I = moment of inertia of specimen cross-section = $\frac{ba^3}{12}$

= 1.63 in.^{4}

$\frac{P}{\Delta_{max}}$ = slope of the straight part of the load deflection curve.

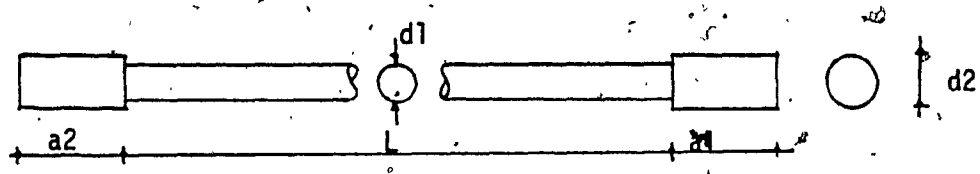

FIG. C.1: TORSION TEST SPECIMEN DIMENSIONS

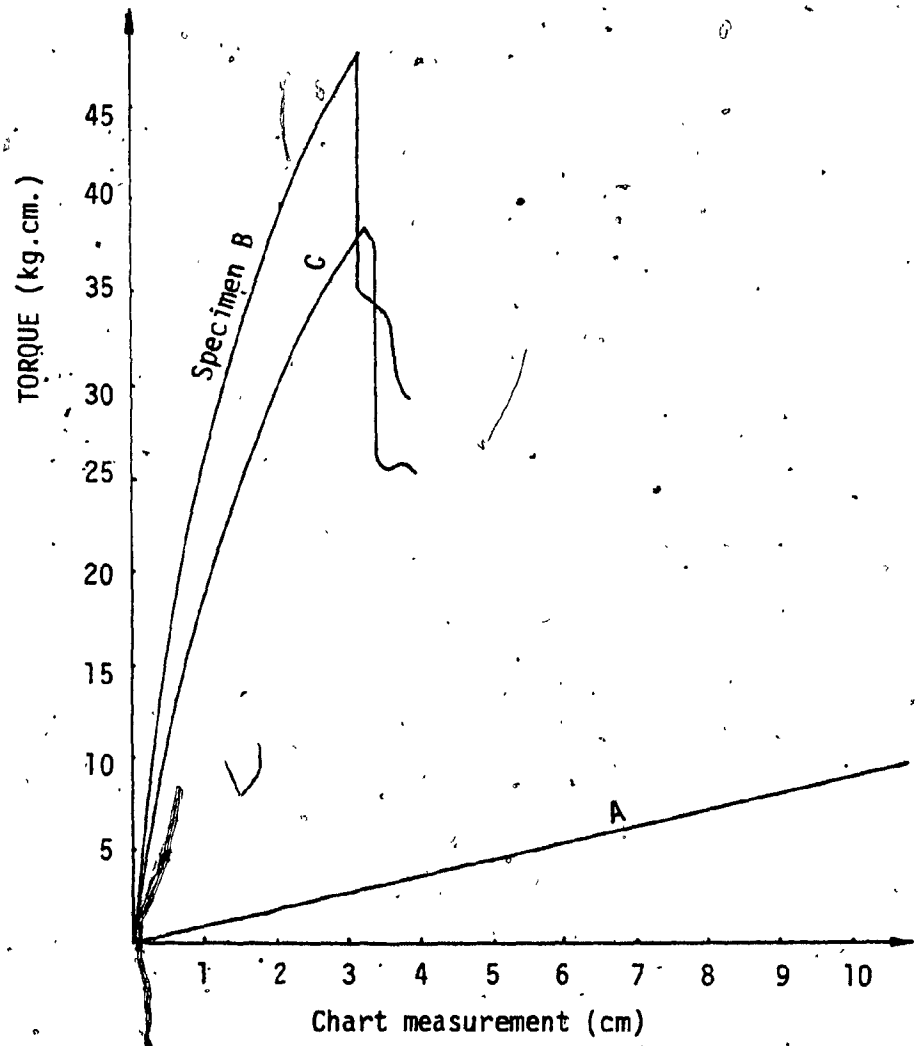

FIG. C.6: TORSION TEST OUTPUT

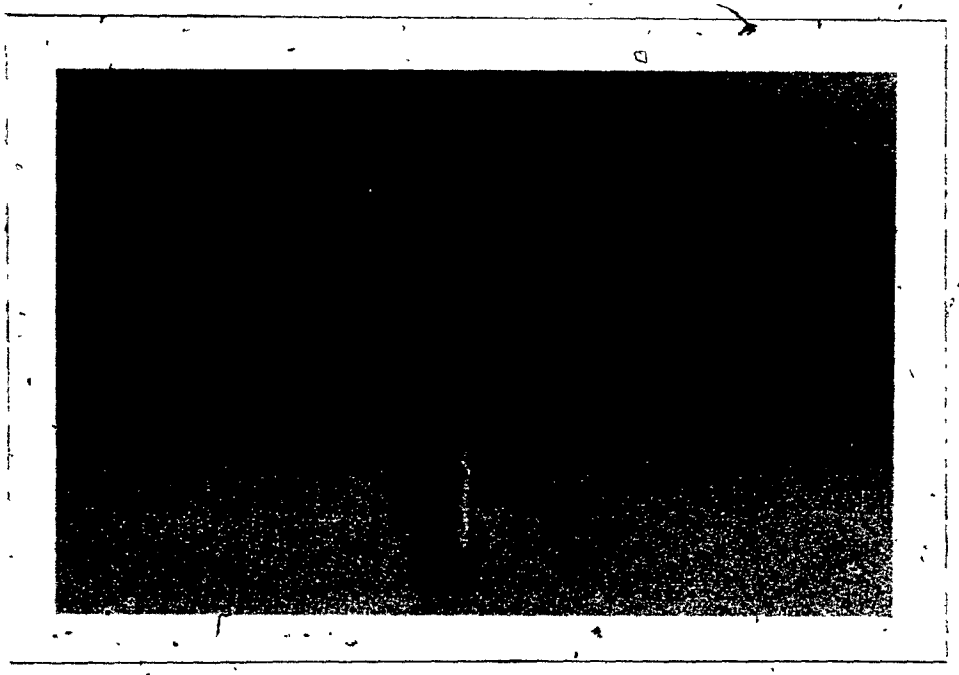

FIG. C.2: TORSION TEST SPECIMEN

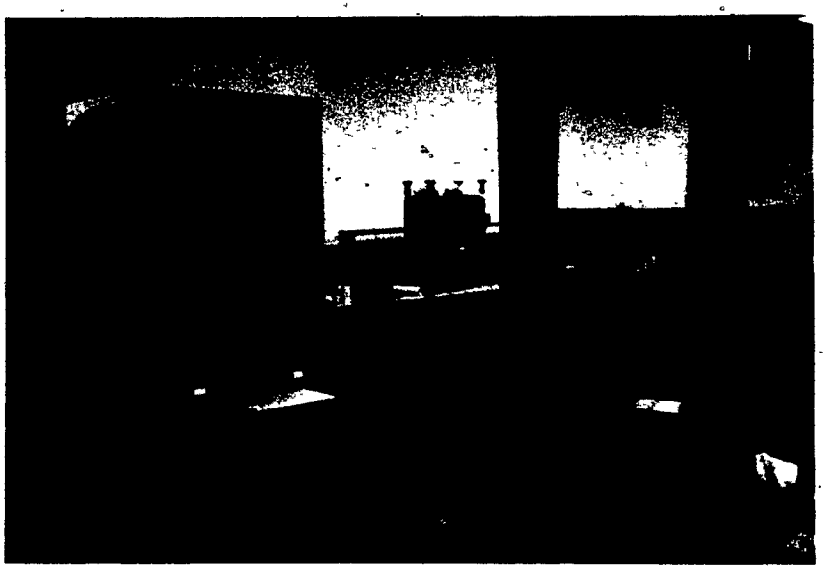

FIG. C.3: INSTRON TESTING MACHINE
USED FOR TORSION TEST

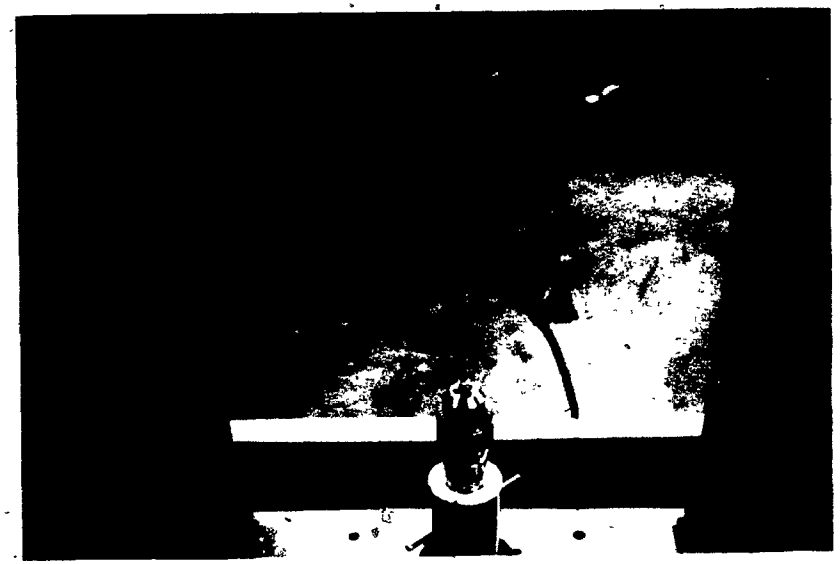

FIG. C.4: TORSION TEST SET-UP

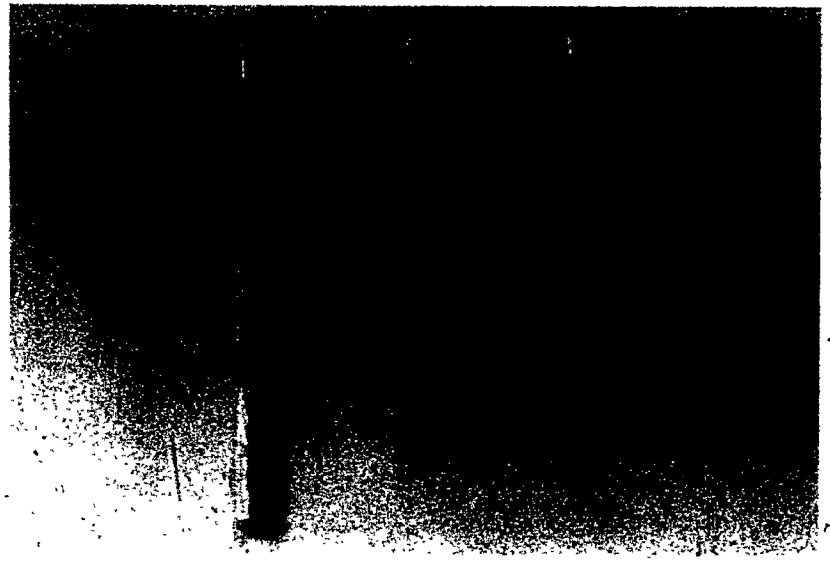

FIG. C.5: SHAPES OF FAILURE OF TORSION TEST SPECIMEN

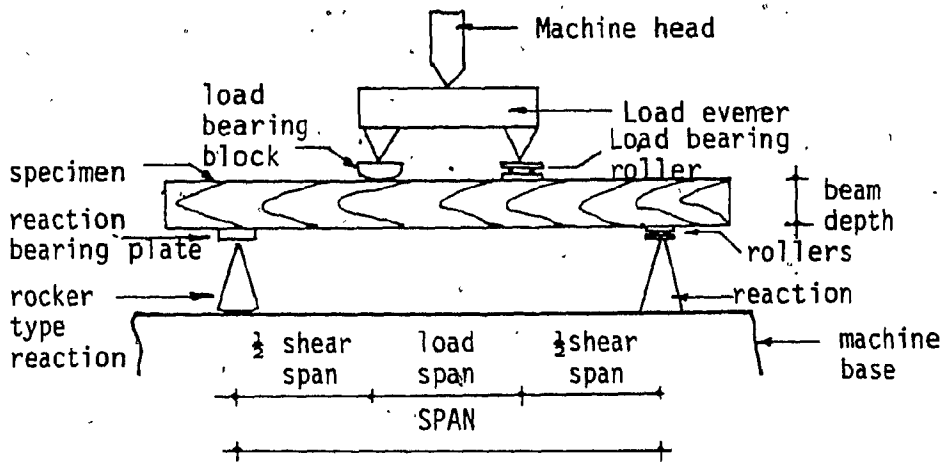

FIG. C.7: FLEXURE METHOD

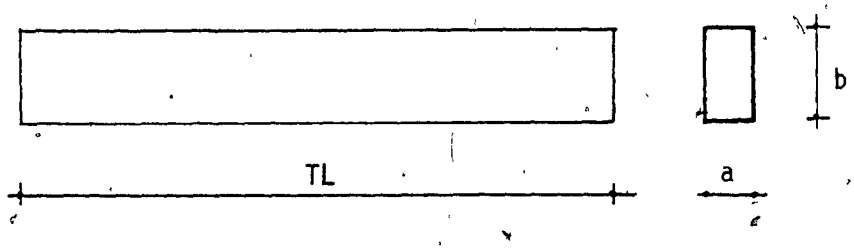

FIG. C.8: FLEXURE TEST SPECIMEN DIMENSION

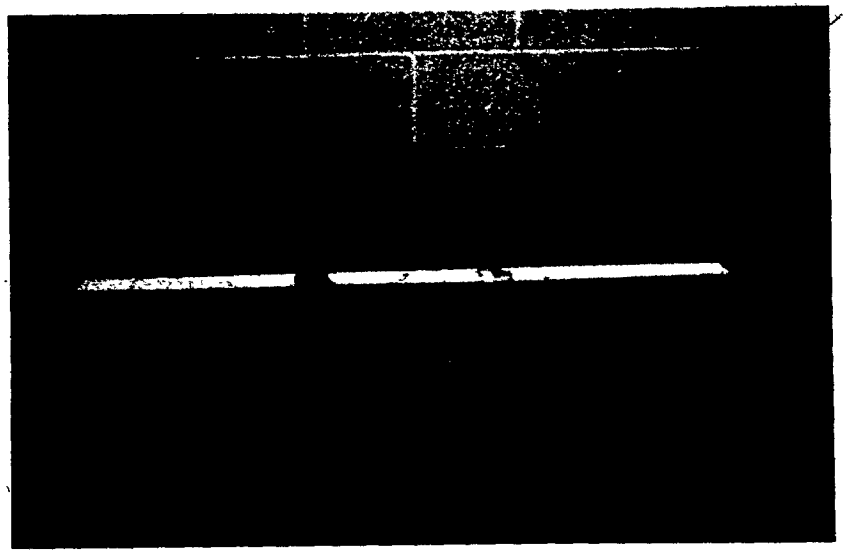

FIG. C.9: FLEXURE TEST SPECIMEN

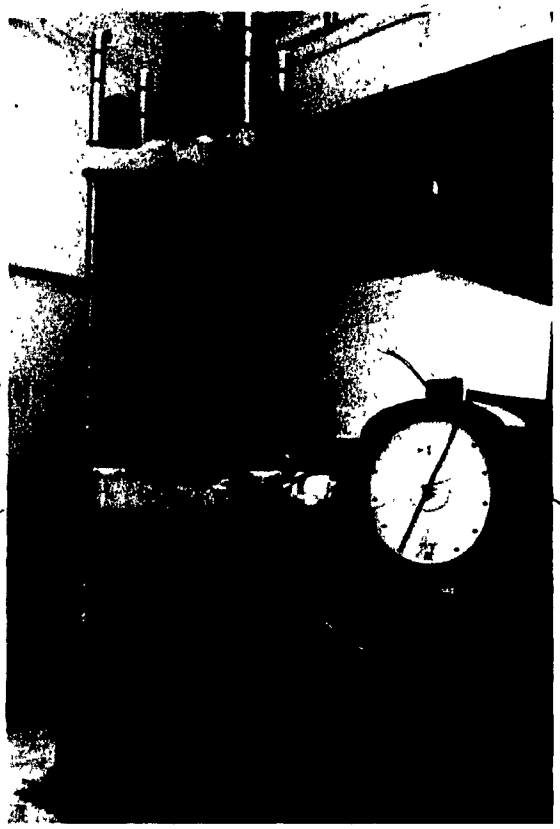

FIG. C.10: TINUS OLSEN TESTING MACHINE USED FOR FLEXURE TEST

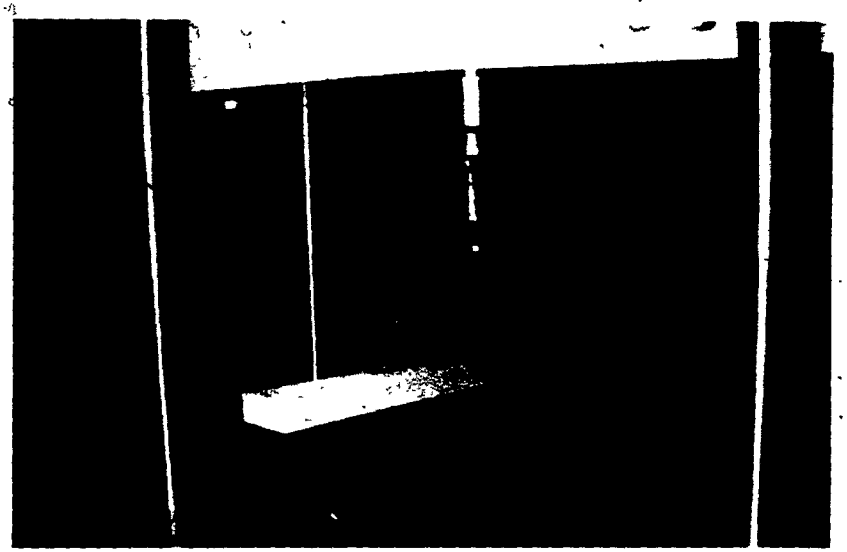

FIG. C.11: TWO POINT LOADS FLEXURE TEST

FIG. C.12: ROLLER SUPPORT OF FLEXURE TEST SPECIMEN

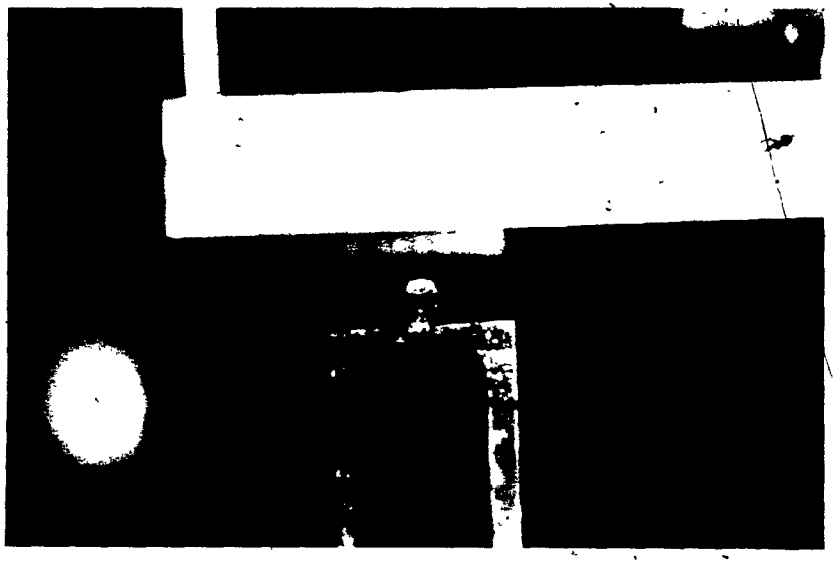

FIG. C.13: HINGE SUPPORT OF FLEXURE TEST SPECIMEN

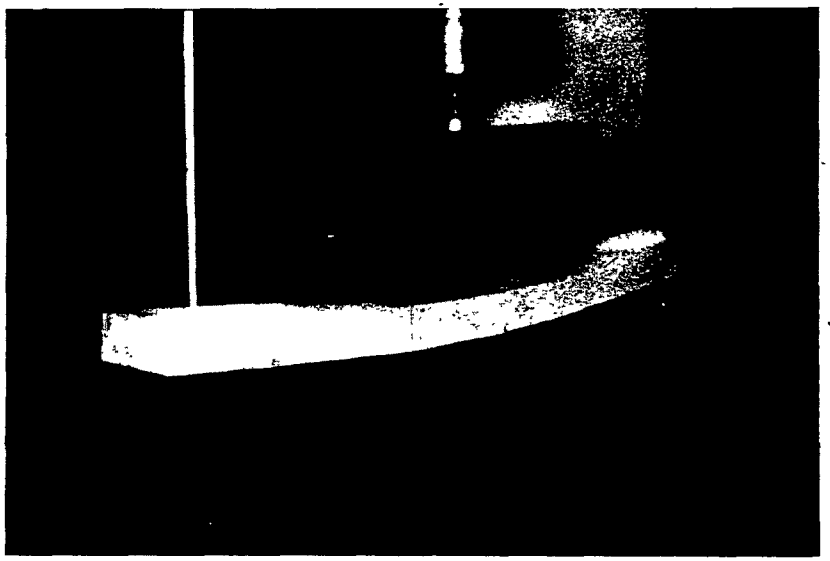

FIG C.14: FLEXURE TEST SPECIMEN
IMMEDIATELY BEFORE FAILURE

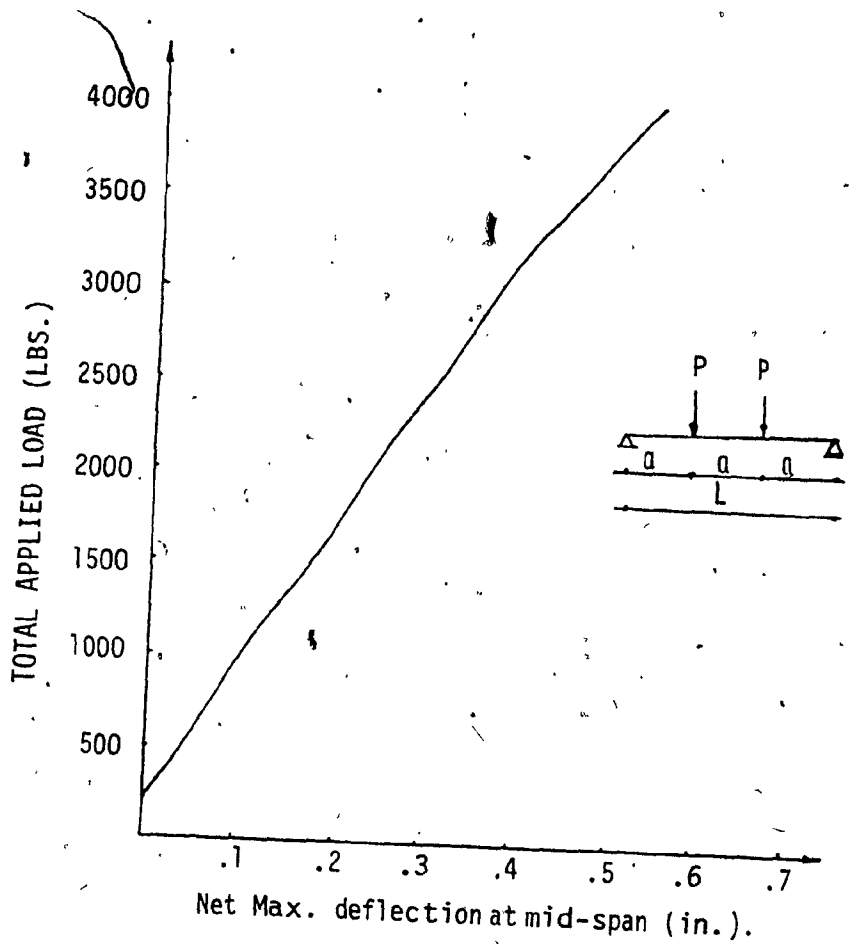

FIG. C.15: LOAD DEFLECTION CURVE